Copyright Warning & Restrictions

The copyright law of the United States (Title 17, United States Code) governs the making of photocopies or other reproductions of copyrighted material.

Under certain conditions specified in the law, libraries and archives are authorized to furnish a photocopy or other reproduction. One of these specified conditions is that the photocopy or reproduction is not to be "used for any purpose other than private study, scholarship, or research." If a, user makes a request for, or later uses, a photocopy or reproduction for purposes in excess of "fair use" that user may be liable for copyright infringement,

This institution reserves the right to refuse to accept a copying order if, in its judgment, fulfillment of the order would involve violation of copyright law.

Please Note: The author retains the copyright while the New Jersey Institute of Technology reserves the right to distribute this thesis or dissertation

Printing note: If you do not wish to print this page, then select "Pages from: first page # to: last page #" on the print dialog screen

ABSTRACT

BIO- MEDICINAL APPLICATION FOR PLASMA ELECTROLYTIC OXIDATION OF METALS

by
Zunjian Yang

Plasma electrolytic oxidation (PEO), a novel method for forming ceramic coatings on metals, has been researched extensively in recent times. By applying high voltage between dielectric thin films, a plasma micro-arc is induced through penetration of breakdown in film boiling layer. Such a method takes advantage of high processing time, low equipment requirement and advanced coating performance.

Titanium alloys, Ti-6Al-4V and pure Titanium Grade 2, are two of most common Titanium alloys in daily use. Both of such Titanium alloys show great potential utilization in bio-medicinal application, especially in implants, for its excellent biocompatibility, high tensile strength, and high elastic modulus. However, in vivo environment is hazardous for metals and alloys. The body fluid is corrosive for metallic implants even for the chemically stable Titanium alloys. Thus methods have been used for surface modification and coating. Plasma electrolytic oxidation has shown its advantage on such demands.

In this thesis, the in vitro corrosion experiment is done on the PEO treated Titanium alloys .The potential of PEO treated metals has few tests in vitro before for bio-medicinal usage. And also the potential dental and implants utilization of PEO treated Titanium alloys can be fulfilled by such analysis and qualified for in vivo test. The surface morphology is analyzed by various of methods in microscopy, electrochemical methods and XRD.

BIO- MEDICINAL APPLICATION FOR PLASMA ELECTROLYTIC OXIDATION OF METALS

by
Zunjian Yang

A Thesis
Submitted to the Faculty of
New Jersey Institute of Technology
in Partial Fulfillment of the Requirements for the Degree of
Master of Science in Materials Science and Engineering

Interdisciplinary Program in Materials Science and Engineering

May 2015

APPROVAL PAGE

BIO- MEDICINAL APPLICATION
FOR PLASMA ELECTROLYTIC OXIDATION OF METALS

Zunjian Yang

Dr. Joseph W. Bozzelli, Thesis Co-Advisor Date
Distinguished Professor of Chemistry and Environmental Science, NJIT

Dr. Reginald P. Tomkins, Committee Member Date
Professor of Department of Chemical, Biological and Pharmaceutical Engineering, NJIT

Dr. Roumiana S. Petrova, Thesis Co-Advisor Date
Senior University Lecturer of Chemistry and Environmental Science, NJIT

BIOGRAPHICAL SKETCH

Author: ZunjianYang

Degree: Master of Science

Date: May 2015

Undergraduate and Graduate Education:

- Master of Science in Materials Science and Engineering,
  New Jersey Institute of Technology, Newark, NJ, 2015

- Bachelor of Science in Chemcial Engineering,
  Shaanxi University of Science and Technology, Xian, P. R. China, 2012

Major: Materials Science and Engineering

为了我爱的人，为了爱我的人
For those I loved, for those who love me

ACKNOWLEDGMENT

I am more than gratefully to appreciate Dr. Roumiana S. Petrova, for all her support and kindness. She is mindful and helpful in research. After a research under her guidance for a year, what I acquired is not only the knowledge but also wisdom in academic.

My special thanks go to Dr. Reginald P. Tomkins and Dr. Joseph W. Bozzelli for join my defense committee, for their support and precious time.

Other thanks go to Dr. Zhonghou Cai from Argonne National Laboratory and John P. Gashinski from Affiliated Engineering Laboratories, Inc. for their help in XRD and SEM.

At last, I am more than appreciated to my senior in laboratory, Linxin Zhu, for all his teaching, guidance and support. He is more than a PhD student, but a role model for me.

TABLE OF CONTENTS

TABLE OF CONTENTS
(Continued)

Chapter **Page**

TABLE OF CONTENTS
(Continued)

LIST OF TABLES

LIST OF FIGURES

LIST OF FIGURES
(Continued)

LIST OF FIGURES
(Continued)

LIST OF SYMBOLS

ω	Angular Frequency Dependent Impendence
V	Voltage
I	Current
ø	Diffraction Angle
µm	Micrometre
Ω	Ohm
F	Capacitance
E_{cor}	Overpotential

LIST OF ABBREVIATIONS

PEO	Plasma electrolytic deposition
HA	Hydroxyapatite
EIS	Electrochemical impedance spectroscopy
SEM	scanning electron microscopy
XRD	X-ray diffraction
CPE	Constant phase element
EDTA	Ethylenediaminetetraacetic acid
APS	Advanced photon source
ANL	Argonne national laboratory
MPY	Mils penetration per year
EDS	Energy Dispersive Spectroscopy

CHAPTER 1

INTRODUCTION

Surface modification has a great impact on material utilization. The surface morphology - interfaces interacting with environment - will affect the behavior of the materials. For bio-materials used in the human body the surface treatment will affect the interaction between implants and body environment [1]. In this thesis, a novel surface treatment technique is discussed for using it in vitro.

1.1 Biomedical Implant

There are three hotspots in contemporary metallurgy research: metallic glass, porous metal and biomedical material. With the development of surgical techniques and understanding of the human body, the demand of novel biomaterials has been increasing. The success of implant operation depends not only on the surgical and therapy procedures but also on the characteristics of the implant material. For a successful implantation, the biocompatibility of the biomaterial, the interactions between implant and human tissue, plays the curial role [1].

Bio-material, commonly consist of polymers, ceramics, stainless steel, pure Titanium or Titanium alloy, Nickel alloy, Cobalt-Chromium alloy, Zinc alloy, Magnesium alloy, Platinum alloy and pure Gold and Gold alloy. The material becomes bio-material by several conditions [1]:

1. Meet the strength requirement of implants.
2. High strength to weight ratio and long elastic region.

3. Chemical stability in body environment.
4. Positive tissue-implant interaction: high adhesion and low immune response.
5. Low negative effect on long term cytotoxicity or hemolysis.

The human body is able to respond to any foreign object which is intruding internal environment. Such reaction is identified as host reaction. The host reaction can be triggered by virus, bacteria, and implants. Host reactions to biomaterials are listed in Table 1.1:

Table 1.1 List of Host Reactions to Biomaterials

Host Reaction	Results
Thrombosis	A blood clot which is induced by the positive charged ions released by implant forms in blood vessel and blocks the circulatory system.
Hemolysis	The unnatural degradation of red blood cells in vivo as the result of hemolysis element intrusion, such as Cr.
Inflammation	The intense immune response to implant triggered by foreign object reaction, an inevitable response for all implants.
Carcinogenesis	The tendency of causing cancer by potential cancer inducing ions released by implants.
Hypersensitivity	The common, mild reaction from immune system to any foreign object to human body.
Systemic Effects	Long term effects such as Alzheimer disease by Al ions released by implant.

Source: [1]

As what is shown above, most of side effect induced by implants is caused by metal ions released by implants. The metal ions released from implant are a primary result of in vivo electrochemical process. Alloys are not stable under in body fluid environment for the metals are most chemical active elements and the in vivo environment is mostly hazard for most alloys. Corrosion in vivo is the most concerned subject when metallic implants are

designed [1].

Corrosion in body fluid, or in vivo corrosion behavior, is one of the most important evaluation points of metallic biomaterial. The corrosion degradation product of implant will flow through the body circulatory system. Certain elements that are released from the implants are potentially harmful for human and it will trigger host reactions in the human body.

The nature of most engineering alloys is chemical active in body fluid environment with a few exceptions. Noble metals, such as Platinum and Gold, are highly stable in human body environment. However, noble metals and its' alloys are not fully satisfying the mechanical behavior requirement of implant, for most noble metals, it will yield under load carrying condition.

There are six groups of engineering alloys which are suitable for biomaterial's requirement: stainless steel, pure Titanium, Titanium alloy, Nickel alloy, Cobalt-Chromium alloy, Zinc alloy, Magnesium alloy.

The first generation biomaterial is stainless steel, it served only as basic function of implant.

The second generation biomaterials are Nickel alloys and Cobalt-Chromium alloys, it has higher corrosion resistance for Nickel, Cobalt and Chromium is self-passive elements. However, those metals are potential toxic for the human body.

The third generation biomaterials are Magnesium alloy and Titanium alloys. The third generation biomaterial takes the advantages of high strength-weight ratio, low side effects to human body, high biocompatibility and more biology functions such as safe-degradable.

The high corrosion resistance and high strength to density ratio of Titanium and its alloys make it an ideal for biomedical utilization. Titanium has the highest specific strength in bulk metals, meanwhile it's a chemical inert element for the ability to form passive layer in oxidation environment [2].

Table 1.2 Mechanical Properties of Titanium Alloy

Material	**Density (g/cm^3)**	**Elastic Modulus (GPa)**	**Tensile Strength (GPa)**	**Yield Strength (MPa)**
Titanium Grade 2	4.5	75	340	900
Titanium Grade 5	4.5	110	550	860

Source: ASM Handbook Volume 2.

1.2 Plasma Electrolytic Oxidation

In 1986, the former Soviet Union sent the space station MIR into space. In order to prolong the endurance of material used on the space station, the concept of plasma electrolytic oxidation was invented. In the first place, this technique was used on Aluminum alloys. With the rapid development of metal surface treatment, such technique has been used for Titanium and Titanium alloys.

The high corrosion resistant and high strength to density ratio of Titanium and its alloys make it ideal for biomedical utilization [1]. However, Titanium has a relatively low surface hardness and low resistance to wear. Also, even Titanium has the relatively high corrosion resistance, the corrosion assist wear and fatigue will still have a great effect on ion release of implants. The need of biomaterial requires surface modification of Titanium

alloys.

Plasma Electrolytic Oxidation (PEO) is one of the suitable processes for surface treatment of bio-material. The ceramic layer created by PEO increases the wear resistance and corrosion resistance of the substrate. However, the potential application of PEO in biomaterial has not been unearthed throughout.

1.3 Hydroxyapatite

There are two major components of human bone: hydroxyapatite (HA) and collagen. The hydroxyapatite, is a natural mineral which chemical composition is $Ca_5(PO_4)_3(OH)$. Together with the collagen, the hydroxyapatite forms the scaffold of human body: bone. Similar to reinforced concrete, hydroxyapatite acts as the concrete while the collagen acts as the steel bar to reinforce the hydroxyapatite [2].

Other than structure element for bone, the hydroxyapatite is also a body friendly coating for biomaterial. As an inorganic salt the hydroxyapatite is chemical stable both in natural environment and in vivo environment. Moreover, the degradation product of hydroxyapatite is Calcium and Phosphorus salt, which is non-toxic for human body in short term or long term. And for the matrix structure of the hydroxyapatite, the bone cells are able to bond to the hydroxyapatite coating by the regeneration of the bone tissue, shown in Figure 1.1. Also, high bio affinity for bone adhesion benefits from its' natural constituent of bone.

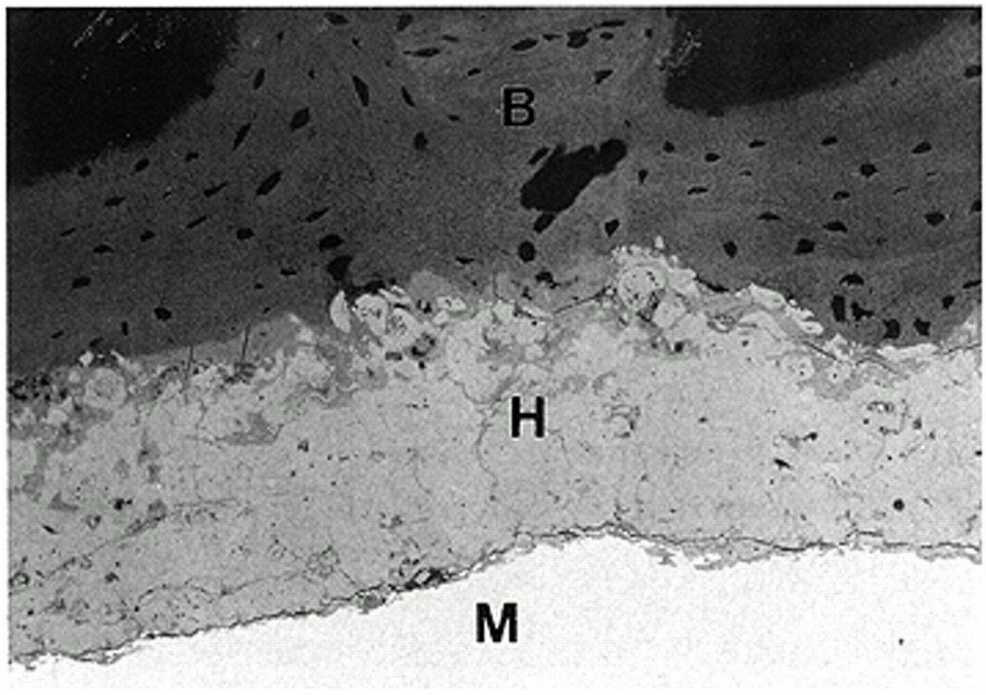

Figure 1.1 Bone affinity of hydroxyapatite coated implant. B: bone; H: hydroxyapatite coating; M: metal.
Source: [3]

The high chemical stability and high bio affinity of hydroxyapatite make it a perfect candidate of coating material for bone implant. In a previous study, the hydroxyapatite coating was finished by sol-gel, thermal spray and etc. However, in those methods, it has certain advantages and disadvantage [3].

The PEO can also be used for depositing HA onto a metal surface. The advantages of the PEO process are shown as follows [4]:

1. High bonding strength.

The nature of plasma chemical will create a high strength bonding. The intense reaction during process results in relatively high bonding strength in bond between coating and substrate. That gives this process an advantage over most sol-gel for the high affinity of coating.

2. Low thermal shear stress

The thermal spray coating is unable to form a thick layer; the thermal spray uses high temperature to ionize atom and deposit it onto coating surface. The thermal expansion between different thicknesses is able to cause shear stress, and thus this will result in cracks, dislocation and coating peel off. During PEO process, the process is undergoing aqua environment and the global reaction is a ‘cold’ process while only local atom level reaction is under ‘hot’ condition.

3. High reaction speed

The entire process takes less than 10 minutes. Fast reaction gives more flexible in production and more economy benefit.

4. Low impurity interference

The plasma spray lacks of pH control during forming thecoating. The structure and chemical constituents is highly depending on the pH. For example, HA has different formation under different pH. The in aqua process of PEO makes it possible for pH control during coating. This reduces the impurity interference for the final product.

1.4 Corrosion and Electrochemical Test

Corrosion, a chemical reaction between material and environment, will gradually destroy the implants. The principle behind corrosion is complex due to the implant facing electrochemical reaction from multiple component electrolyte under body temperature [4].

There are several kinds of corrosion in general [5].

1.4.1 Uniform Corrosion

Uniform corrosion is a general corrosion which takes place at the surface between metal and environment. It's the most commonly observed corrosion and occurs at most corrosion scenario. In most corrosion case, uniform corrosion occurs along with other forms of corrosion, and the effect of different corrosions will effect with each other [5]. Shown in Figure 1.2.

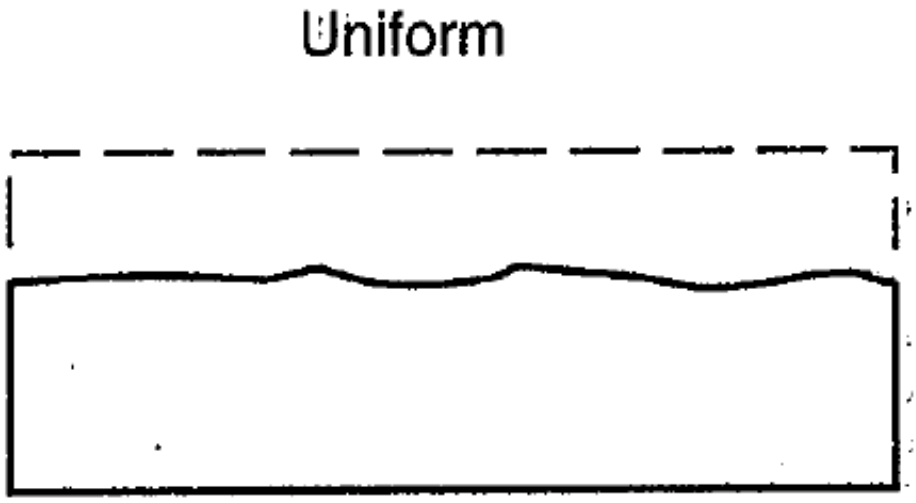

Figure 1.2 Uniform corrosion.
Source: [5]

1.4.2 Galvanic Corrosion

Galvanic corrosion occurs at two metals or alloys which have different corrosion potential. In galvanic corrosion, the metal or alloy pairs will form a cell which the noble metal will be protected and the active metal will be corroded. The order that metal whether will be corroded is listed as Galvanic series [5]. Shown in Figure 1.3.

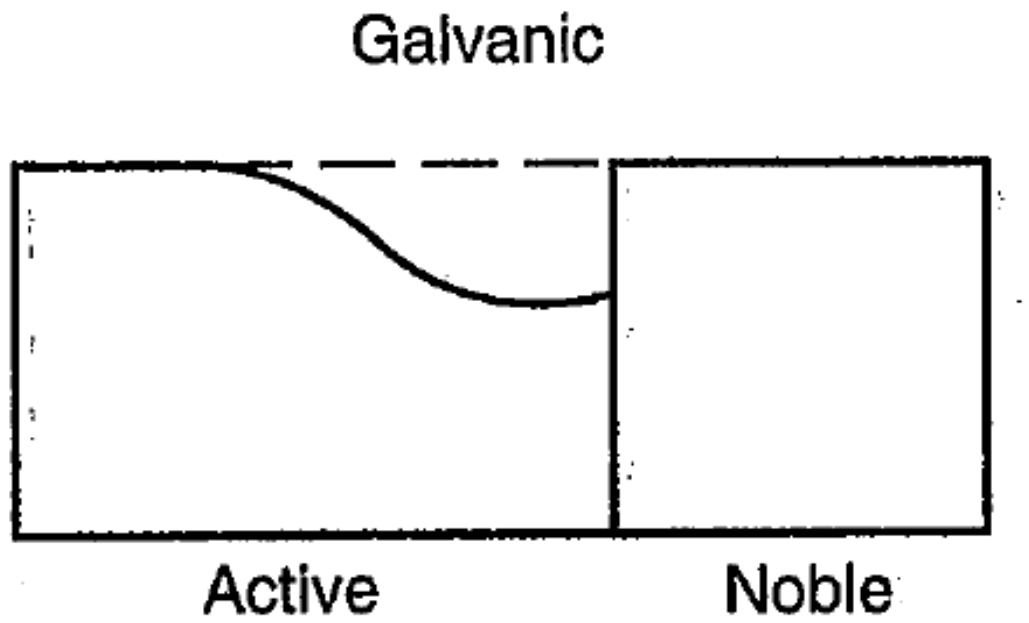

Figure 1.3 Galvanic corrosion.
Source: [5]

1.4.3 Crevice Corrosion

Crevice corrosion can be described as hole-effect corrosion. As a small volume space is created in the metal or alloys, the water or other solution is filling the small space. As the corrosion takes place in that small space, the hydrogen is exhausted and more negative charged ion will enter the space.

This process creates an enrichment region of ions in liquid of that small space. With a rise in concentration of ions, the speed of corrosion reaction increases significantly [5].

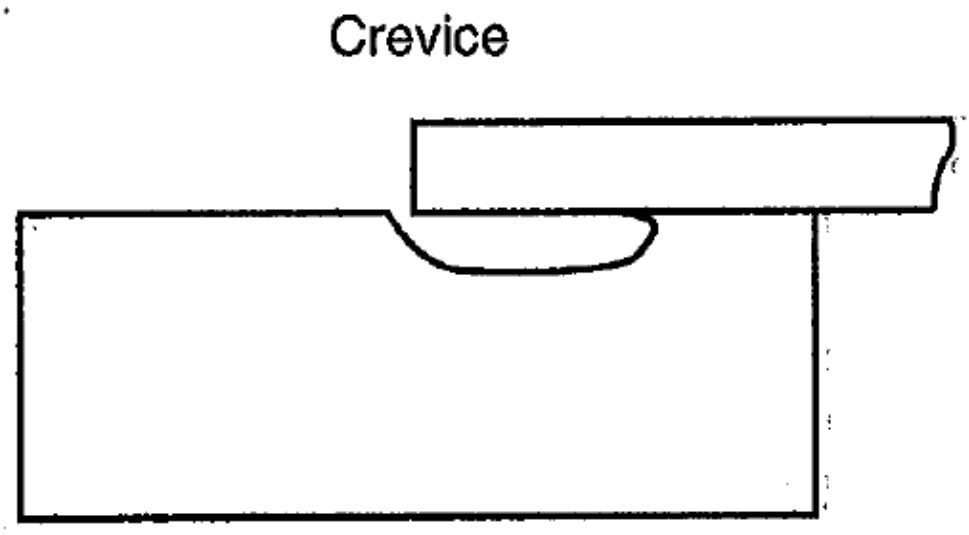

Figure 1.4 Crevice corrosion.
Source: [5]

1.4.4 Pitting Corrosion

Pitting corrosion often happens on protected alloys. The corrosion attacks crack or damaged point on the protect surface. As the uneven corrosion going on, a series of pits will be formed on the surface of the alloys. The theory behind pitting corrosion is similar with crevice corrosion, thus the pitting corrosion will be digging into the surface of alloys. At the pitting surface, a wide spread pitting corrosion hole will be found [5]. It's shown in Figure 1.5.

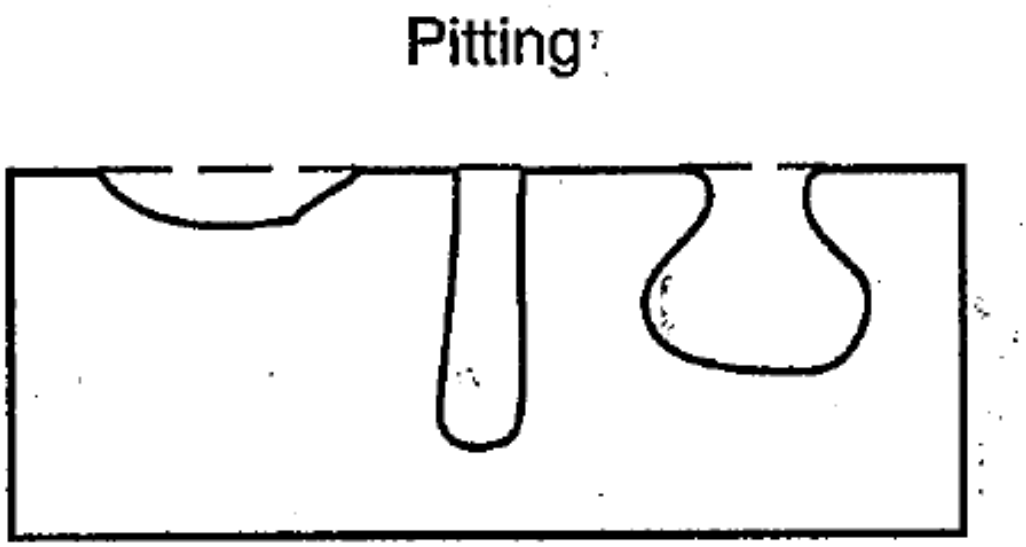

Figure 1.5 Pitting corrosion.
Source: [5]

1.4.5 Environmentally Induced Cracking

Corrosion is able to cause brittle failure in ductile material, which is a combination effect of corrosion effect and applied stress. There are three types of environmentally induced cracking: stress corrosion cracking, corrosion fatigue, hydrogen-induced cracking. As the static or cyclic stress is applied to the surface, a small crack and high diffusivity zone is created for accelerating the corrosion rate and the corrosion will also affect the mechanical behavior of alloys [5] as shown in Figure 1.6.

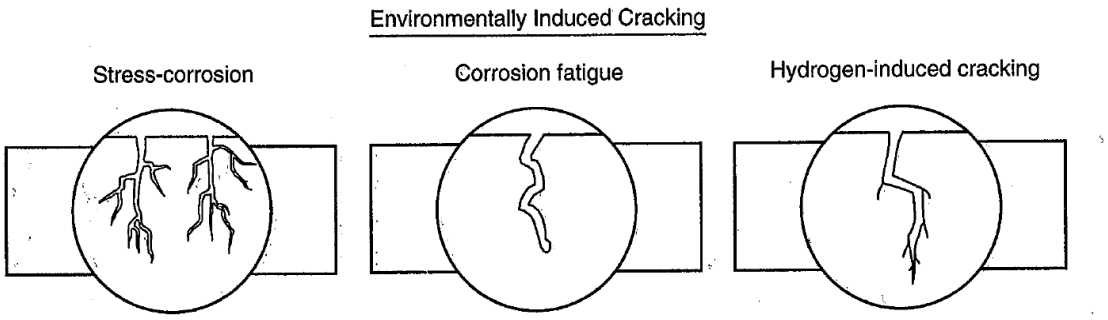

Figure 1.6 Environmentally induced cracking.
Source: [5]

1.4.6 Intergranular Corrosion

The certain elements depletion in intergranular region, such as passivating elements or protecting elements, will result in less corrosion resistance of intergranular region. In alloys the intergranular corrosion is usual problems for most alloys consist of passivating elements such as Chromium. During certain tailoring process such as heat treatment, the Cr could be depleted by diffusion as shown in Figure 1.7.

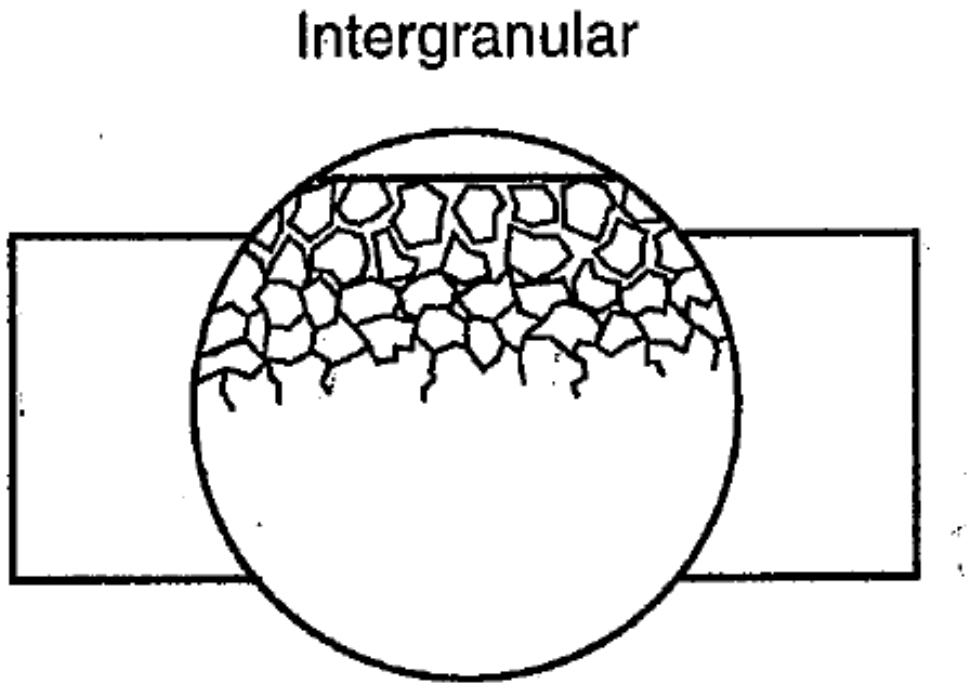

Figure 1.7 Intergranular corrosion.
Source: [5]

1.4.7 De-alloying and Dezincification

In the alloy which contains active elements for corrosion protection, the de-alloying is able carried out by depletion of protect elements. More reactive element is likely to react with the corroding media, the protecting elements moves to the corrosion area of alloys by diffusion thus cause the depletion. The most significant example is the dezincification of brass [5] as shown in Figure 1.8.

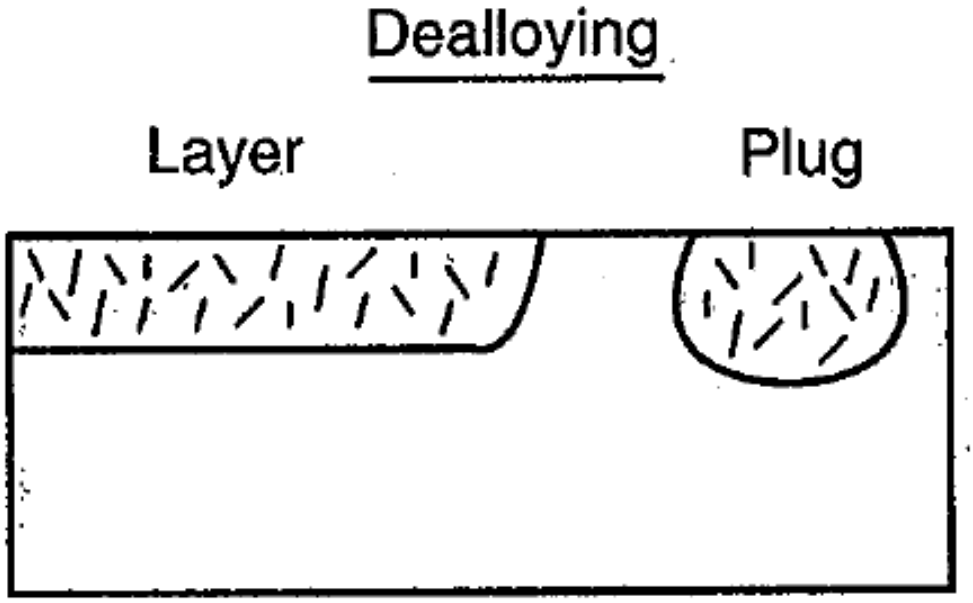

Figure 1.8 De-alloying.
Source: [5]

1.4.8 Erosion-Corrosion and Fretting

High speed fluid washing combined with electrochemical reaction is able to damage the alloys than by any of the effect if alone. As the high speed fluid will remove the disintegrated part of material, the passive layer will be peeled off thus result in a new routine. An erosion-corrosion is the highest rate corrosion process, where both mechanical and electrochemical take place [5], which is shown in Figure 1.9.

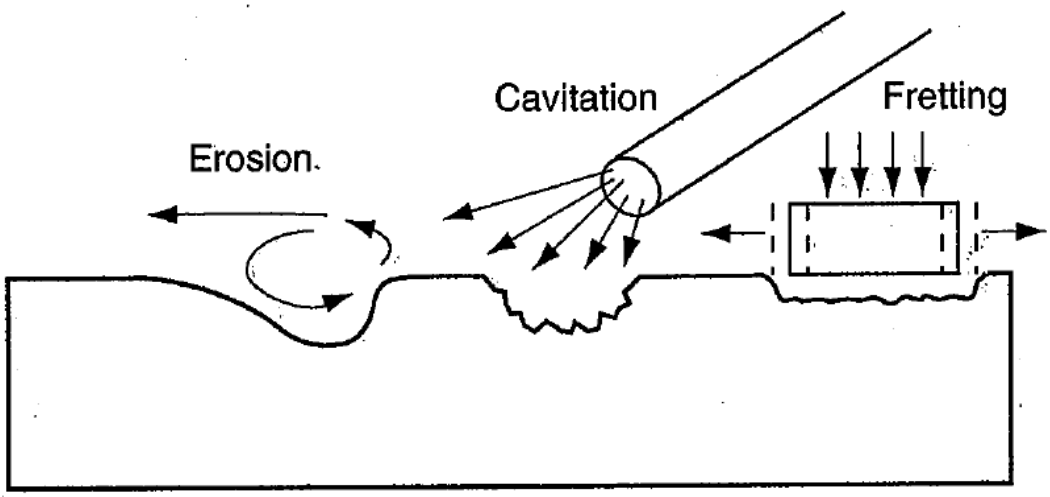

Figure 1.9 Erosion-corrosion and fretting.
Source: [5]

1.5 Hank Solution

There are numbers of balanced salt solutions which are able to simulate internal environment, such as Alsever's solution, Phosphate buffered saline, TRIS-buffered saline Tyrode's balanced salt solution and Hank's balanced salt solution. Hank's balanced salt solution, or Hank solution for short, is a solution to simulate physiological inner human body environment by create a similar pH and ions concentration. It's widely used for simulation for reaction between implants and body fluid [4].

The Hank solution contains Calcium chloride, Potassium chloride, Potassium phosphate monobasic, Magnesium chloride, Magnesium sulfate, Sodium chloride, Sodium bicarbonate, Sodium phosphate dibasic, Glucose, and Phenol red. The formula of Hank solution is to duplicate same variety and concentration of ions in extracellular fluid, and by doing this creates a similar electrochemical extracellular environment in vitro.

In this thesis, Hank's solution is selected as the simulation fluid for the experiment

of corrosion in vitro. For decades the Hank's solution had been used for biomedical material science and makes it major solution for body fluid related experiment.

The pH and ions plays important role in vitro corrosion evaluation, as the pH affects the speed of reaction between solution and metal, and ion effect the kinetic of reaction. The Hank's solution consists most of ions and salt and the same pH in internal body fluid, which makes it prefect as a candidate for simulation corrosion.

Table 1.3 Chemical Composition of Hank's Solution

Component	Concentration (gm/L)
Calcium Chloride ($CaCl_2$)	0.14
Potassium Chloride (KCl)	0.40
Potassium Phosphate Monobasic (KH_2PO_4)	0.06
Magnesium Chloride ($MgCl_2$-$6H_20$)	0.10
Magnesium Sulfate ($MgSO_4$-$7H_2O$)	0.0
Sodium Chloride (NaCl)	8.00
Sodium Bicarbonate ($NaHCO_3$)	0.35
Sodium Phosphate Dibasic (Na_2HPO_4)	0.048
Glucose	1.00
Phenol Red	0.01

Source: [6]

1.6 Electrochemical Test

In order to evaluate the corrosion resistance of material in certain solution, the electrochemical test is carried out by an electrochemical workstation. There are two tests are to be carried out: potential dynamic and electrochemical impedance spectroscopy [7][8].

The electrochemical test is carried out by Princeton Electrochemical workstation

2263(PARSTAT 2263). The setup of the electrochemical test is shown in Figure 1.10. The sample, as working electrode, is immersed in an electrolyte while connected to the power supply. The reference electrode is also immersed close to the working electrode, and a solution bridge, Luggin probe, is installed to eliminate potential difference caused by solution between the working and reference electrode. At the other side of the cell, the counter electrode, or the auxiliary electrode is immersed into the electrode.

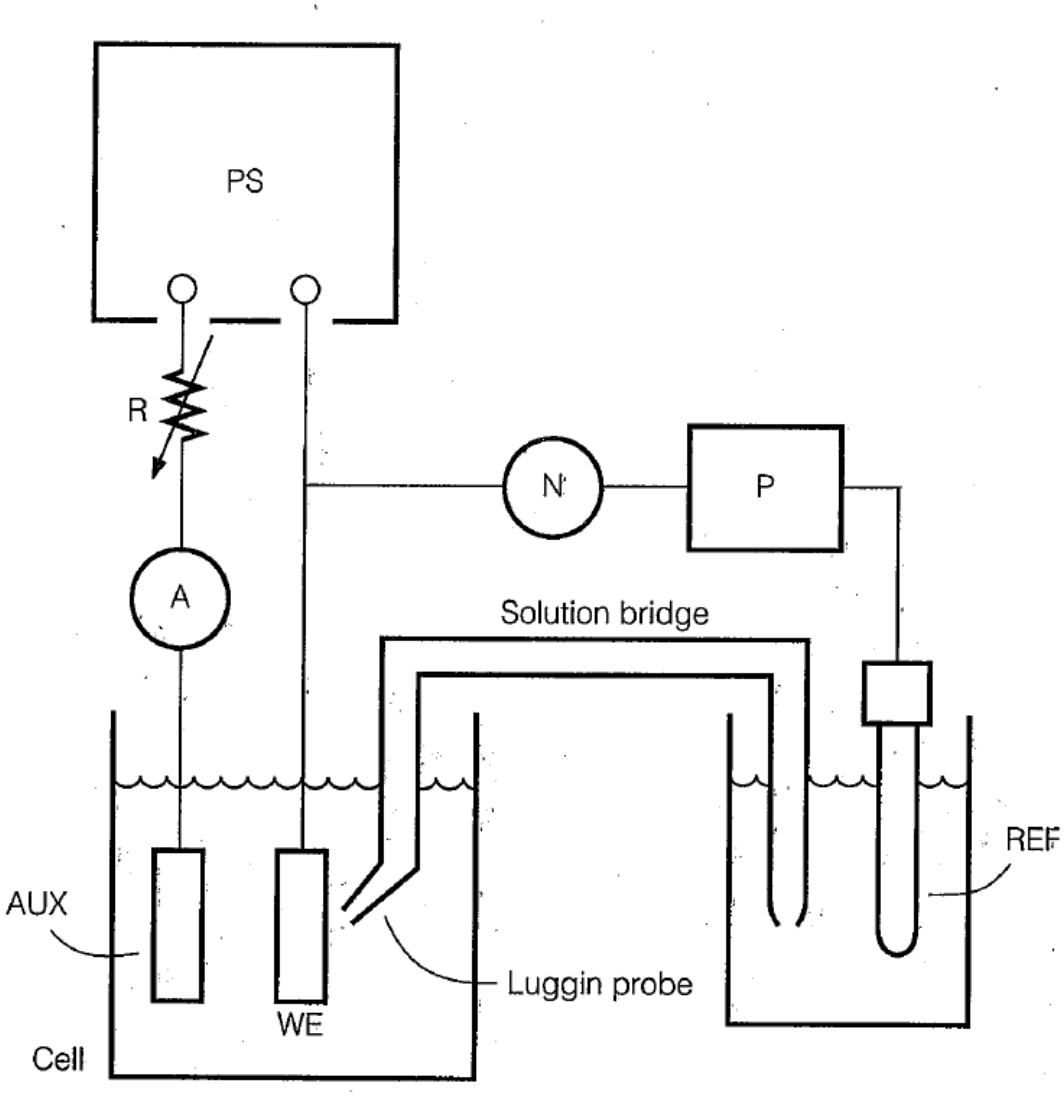

Figure 1.10 Schematic electrochemical experimental setup.
Source: [7]

In this thesis, a silver-silver chloride electrode with saturated potassium chloride is selected as reference electrode, shown in Figure 1.11. The silver-silver chloride electrode has a silver bar in the center as coated by silver chloride. The solution of a silver-silver chloride electrode is saturated potassium chloride electrolyte. The silver-silver chloride electrode has a standard potential of 0.222 V. The reason for choosing silver-silver chloride electrode is the high stable in most experimental environment and the low temperature coefficient of -4.3×10^{-4} V/℃ [5].

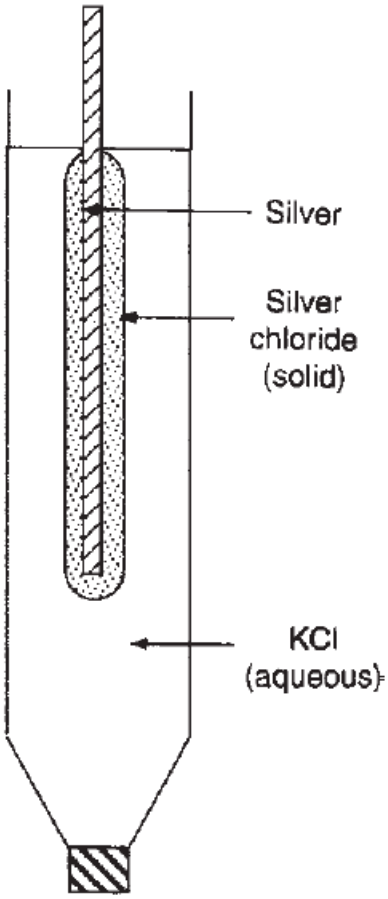

Figure 1.11 Structure of silver-silver chloride electrode.
Source: [5]

1.6.1 Tafel Plot

In the nature of corrosion, there are two parts of half-cell reaction, anodic reaction of metal which is an oxidation reaction, and cathodic reaction of electrolyte, which is a reduction reaction [6]:

$$M\text{-}e^- = M^+ \qquad e_{M/M}{}^{2+}$$

$$2H^+ + e^- = H_2 \qquad e_{H^+/H2} \tag{1.1}$$

Where the M stands for metal element and e stands for free electrons. $e_{M/M}{}^{2+}$ and $e_{H^+/H2}$ are the electrical potential of oxidation of metal and reduction of hydrogen, and they combined together corrosion potential can be calculated.

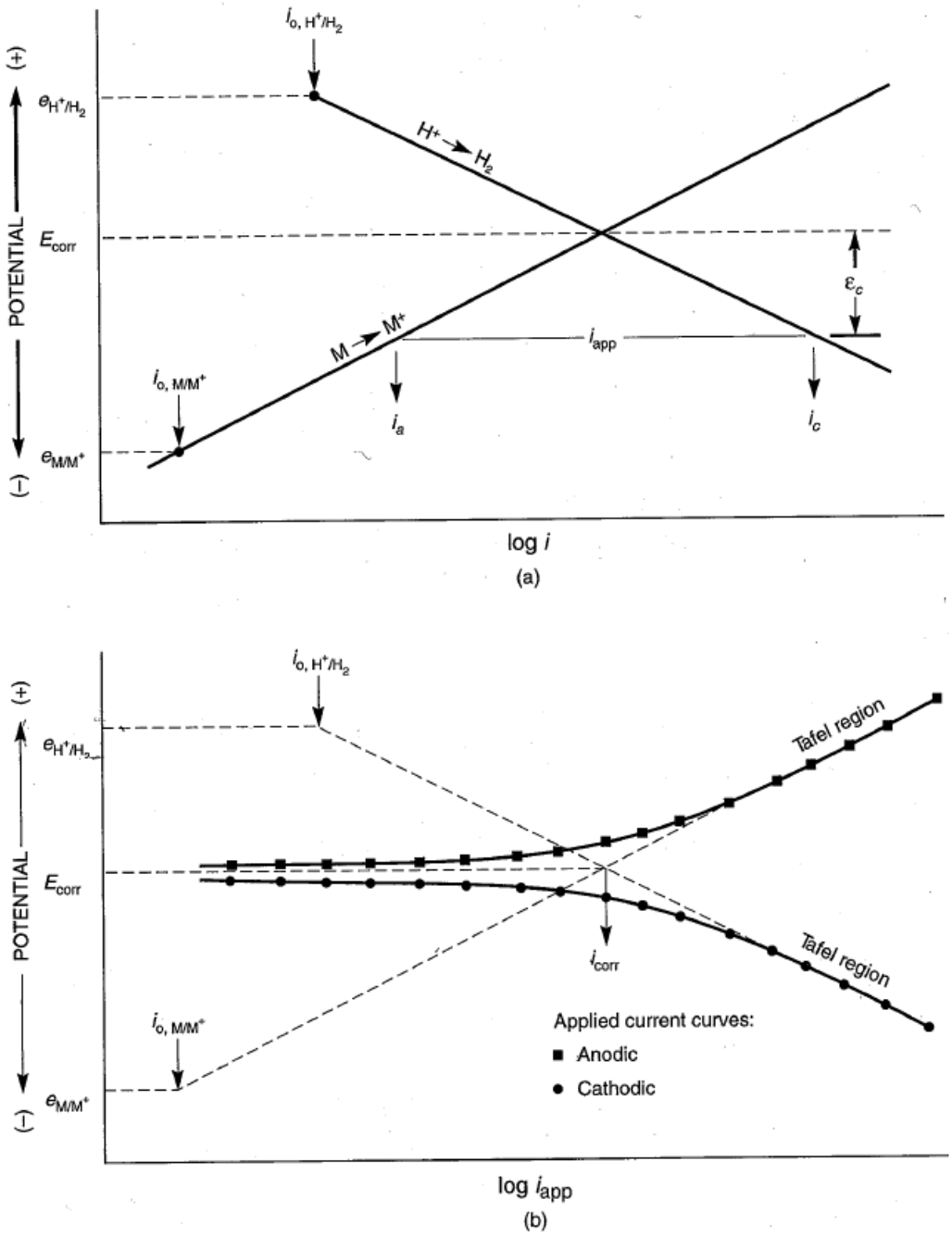

Figure 1.12 (a) Current density, i_{app}, applied to corroding electrode of E_{cor} and i_{cor}, causing cathodic overvoltage of ε_c. (b) simulated experimental polarization curves derived from (a.).
Source: [5]

As the voltage applied to the cell increases, the electrolyte - sample interface is going through two polarization procedures. In the low voltage, the cathodic polarization

takes place first, as the hydrogen reduction play the major role in electrochemical reaction. As with the voltage increased, the total current is gradually dropped to the minimum point, and the reduction and oxidation reaction reaches equilibrium point. As that point the sum of cathodic polarization and anodic polarization are at equal point and the net current exchange reach valley point. The current and voltage at such point is to be identified as E_{corr} and I_{corr}. After the corrosion potential point, the anodic polarization take place, and the metal oxidation act as the major reaction, and the current increased along with the voltage increasing [6].

After the Tafel region, the anodic polarization often shows a typical passive curve, which the net current hold still while the voltage increasing. Such curve is the result of metal oxide layer formed on the surface of metal. Such layer acted as inhibitor of chemical reaction, thus prevents the further reaction of oxidation.

1.6.2 Electrochemical Impedance Spectroscopy

As to exam the coating layer formation, the electrochemical impedance spectroscopy (EIS) is one of the candidates for such purpose. The schematic view of experimental setup of electrochemical impedance spectroscopy is shown in Figure 1.13. With the same setup in Tafel plot of cell setup, the current response of alternating voltage is recorded by computer.

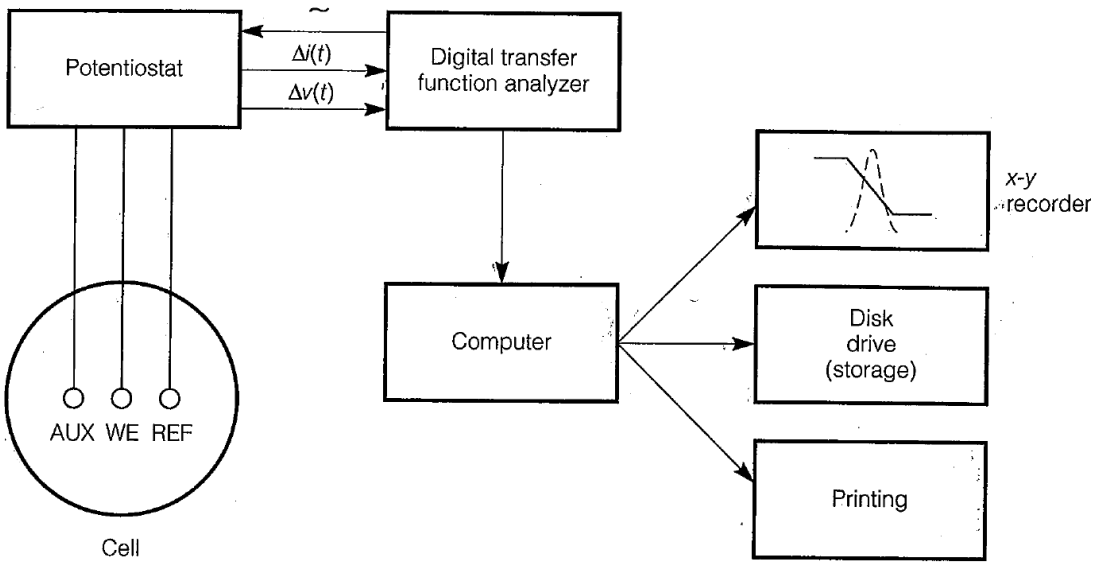

Figure 1.13 Schematic instrumentation for conducting electrochemical impedance spectroscopy.
Source: [8]

By using alternating current, a sinusoidal alternating potential signal is applied to the sample. By recording the current which is responding to the sinusoidal voltage change, angular frequency dependent impedance is recorded, shown in Figure 1.14.

$$Z(\omega) = V(t)/I(t) \qquad (1.2)$$

Where the Z (ω) stands for angular frequency dependent impedance, V(t) and I(t) stand for the time-dependent voltage and current density.

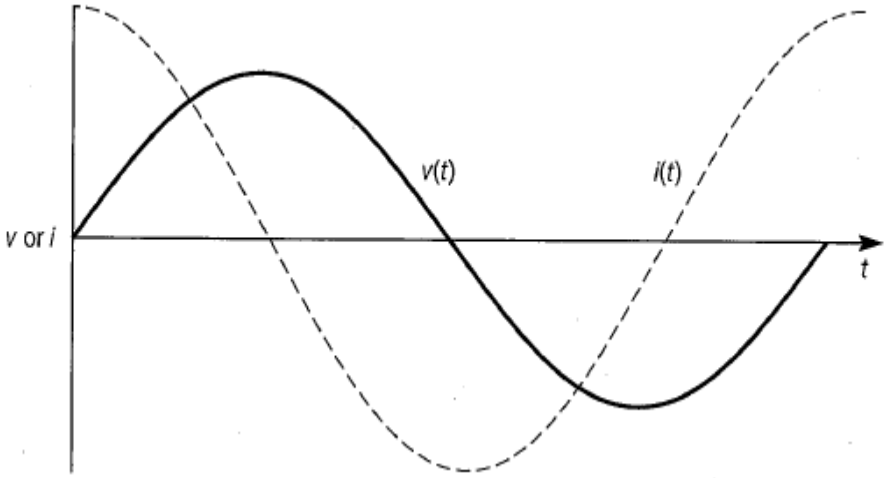

Figure 1.14 Current response, I, to a sinusoidal potential signal, V, for a capacitor.
Source: [8]

As for the angular frequency dependent impedance, there are two items in Z (ω), the real term Z` (ω) and the imaginary term Z`` (ω) [8]:

$$Z(\omega) = Z`(\omega) + Z``(\omega) \tag{1.3}$$

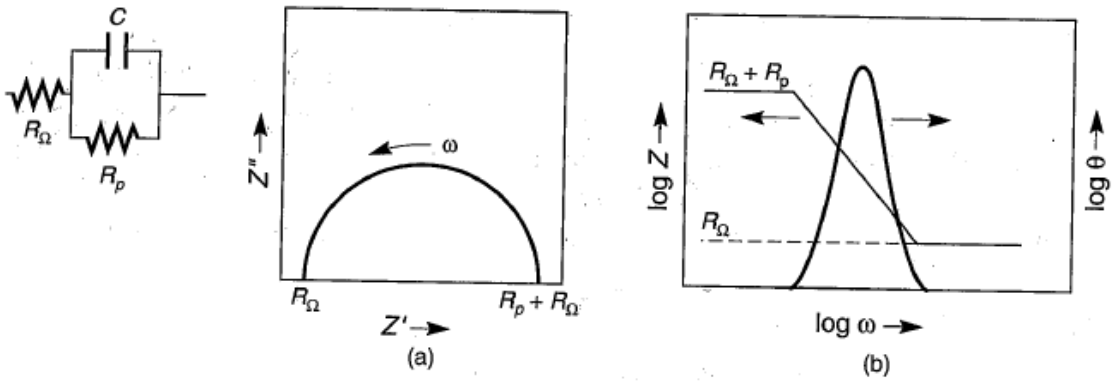

Figure 1.15 Data display for electrochemical impedance spectroscopy for a corroding electrode simulated by parallel-connected resistance R_p and capacitance C. (a) Nyquist plot; (b) Bode plot.
Source: [8]

By analyzing results of the angular frequency dependent impendence, the structure of coating can be inferred.

There are several electronic components can be presumed from the Nyquist plot. A typical electronic component is shown in Figure 1.16.

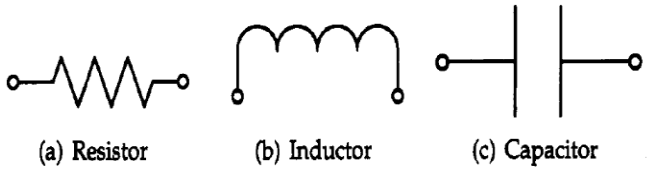

Figure 1.16 Three typical electronic components of EIS.
Source: [8]

The relationship between voltage and current in resistor can be expressed as follows:

$$V(t)=RI(t) \qquad (1.4)$$

Where the I is the current response of altering voltage, V is the voltage and L stand for the resistance of the resistor.

The linear relation between voltage and current indicates the resistor represents a current which is proportional to potential different. Such behavior is the conduction by water or electrolyte. In another word, the resistor can be defined as potential drop on sample surface or leaking in coating, for conducting by electrolyte.

The relationship between voltage and current in inductor can be expressed as follows [8]:

$$V(t)=L\frac{dI(t)}{dt} \quad (1.5)$$

Where the I is the current response of altering voltage, V is the voltage and L stand for the inductance of the inductor.

As for the steady state, the inductor is a conducting wire and can be treated as short circuit. While in the alternate voltage, the inductor will create an inductive reactance which is an electrical against the voltage applied.

The relationship between voltage and current in capacitor can be expressed as follows [8]:

$$I(t)=C\frac{dV(t)}{dt} \quad (1.6)$$

Where the I is the current response of altering voltage, V is the voltage and C stand for the capacitance of the capacitor.

A capacitor shows a nonlinearity relation between current and voltage, as its electrical nature is a dielectric film. In the steady-state condition, it can be considered as an open circuit which has no conductivity. However as the alternate voltage is applied the dielectric film ill respond to the changing in voltage which creating a phase difference current while responding voltage change.

Also, there are serval imaginary components introduced to fit the EIS data:

Constant phase element, an element that represents an imperfect capacitor and which shows behavior of both a capacitor and a resistor [8]. The structure is shown in Figure 1.17:

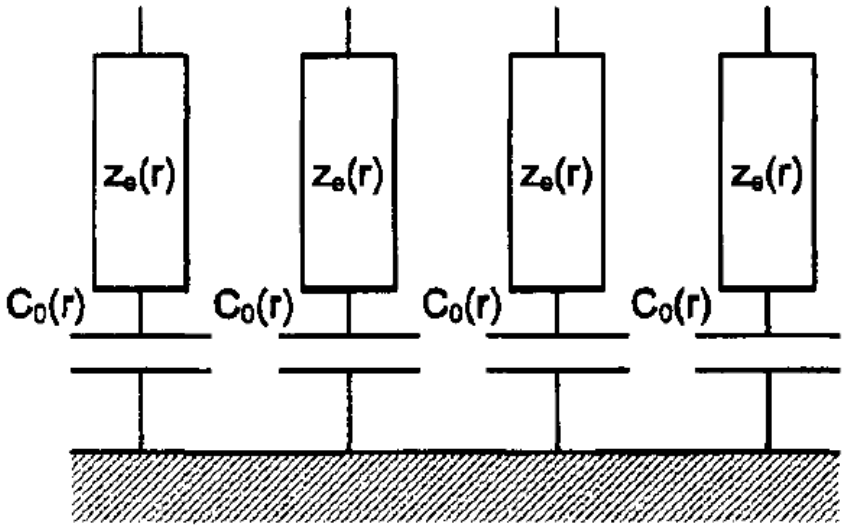

Figure. 1.17 Structure of constant phase element.
Source: [8]

This component is to simulate a diffusion zone near or at the electrolyte -metal surface. The angular frequency dependent impendence of constant phase element can be expressed as follows [8]:

$$Z(\omega)=R_e+\frac{1}{Q(j\omega)^{\alpha}} \quad (1.7)$$

In equation (1.7), the parameters α and Q are independent of frequency. When a = 1, Q has units of a capacitance, i.e., F/cm2, and represents the capacity of the interface. When a ≠ 1, Q has units of sa/Ωcm2 and the system shows behavior that has been attributed to surface heterogeneity or to continuously distributed time constants for charge-transfer reactions. Independent of the cause of CPE behavior, the phase angle associated with a

CPE is independent of frequency [8].

When α=0, the constant phase element is a resistor, and when α=1, the constant phase element is a capacitor.

What can be inferred from the result of the EIS data is the micro structure by conducting electrical components in certain arrangement.

An example is shown in Figure 1.18.

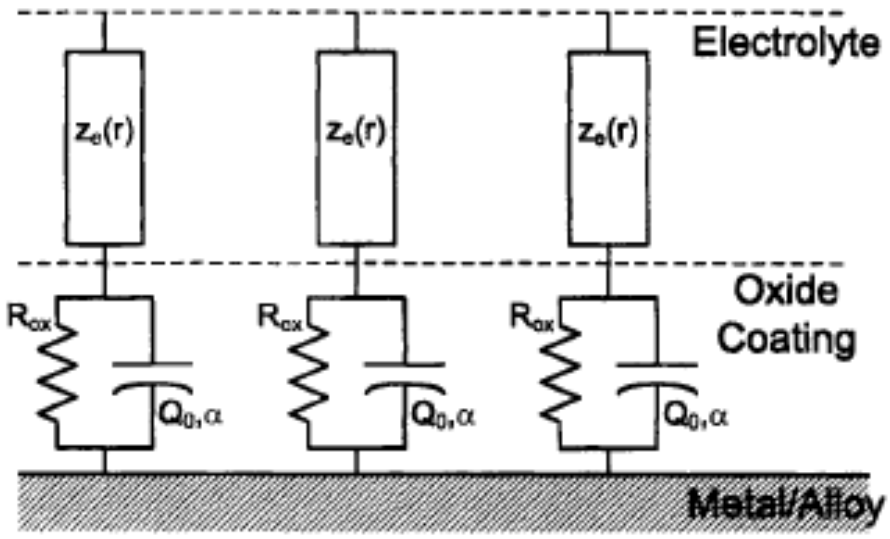

Figure 1.18 Structure of example.
Source: [8]

In this example, an electrolyte layer which electrical conduction is carried by ions in water is represented as constant phase element. The oxide coating is represented by a parallel connected resistor and capacitor.

For the resistor is the closed circuit of conducting electrolyte, and the capacitor is an open circuit of oxide layer, the parallel of resistor and capacitor indicate a partially coating surface, for those two components take effect simultaneously.

1.7 Summary

In this thesis, two metal substrates are selected as candidates for biomaterial: Titanium Grade 5, known as Ti-6Al-4V, and Titanium Grade 2.

Ti-6Al-4V is the most widely used Titanium alloy, also a common biomaterial for biomedical implant such as bone replacement, hip replacement, cardiac scaffold and artificial tooth & screw, will be used in this thesis, for its potential utilization of PEO.

Titanium Grade 2 will be also used in this thesis. For its' low elastic modulus and close to the elastic modulus of bone, the Titanium Grade 2 is able to reduce the stress shielding effect [1].

The surface treatment of samples is shown in Table 1.4.

Table 1.4 List of Samples

Material of Samples	Surface Treatment
Titanium Grade 2	Polished to Ra 4
Titanium Grade 5(Ti6Al4V)	Polished to Ra 4
Titanium Grade 5 with oxide coating	PEO oxide coating
Titanium Grade 5 with HA coating	PEO coating with HA

A number of tests will be performed in order to examine the property of material, including its surface microstructure and morphology.

The list of test is shown in Table 1.5.

Table 1.5 List of Test

Test	Result
Optical microscope	Surface morphology
SEM	Surface microstructure and element distribution
XRD	Crystallography and element distribution
Electro-chemical	Corrosion resistance

CHAPTER 2

SAMPLE PREPARATION

The samples which are going to be tested are treated by Plasma Electrolytic Oxidation process. The sample's substrate used for PEO are Titanium Grade 5, for which the method of PEO is sophisticated [9][10][11][12].

2.1 Pre-Process Procedure

The samples for PEO process are as-roll Titanium Grade 5 plate. At first the samples will be polished to mirror surface by Allied Tech METPREP 3 polishing machine, then rinsed by alcohol. The oxide thin layer will be carefully removed during polishing, since the oxide thin layer will affect the chemical reaction during PEO process. The sample will be cut into 30mm x 30mm square.

2.2 Plasma Electrolytic Oxidation

Plasma electrolytic oxidation, or micro-arc oxidation, is a process using plasma arc breakdown between a dielectric film boiling layer, which is created by electrical potential different, to carry passive element onto the surface of substrate and thus form a dense and thick chemical inert ceramic layer. The ceramic layer is wear-resistant and chemical inert, which will enhance the durability and surface hardness of metallic substrate.

The setup of equipment for plasma electrolytic oxidation is shown in Figure 2.1. The metal substrate will be immersed in the electrolyte. A set of wire is attached to the substrate from a cell which is able to provide voltage ranging from 0V to 500V. The metal

substrate will be connected to anode and a counter electrode will be connected to cathode. In this experiment, graphite electrode will be used as counter electrode, for its chemical inert and high conductivity. The power supply will create an electrical potential difference between electrolyte and metal substrate.

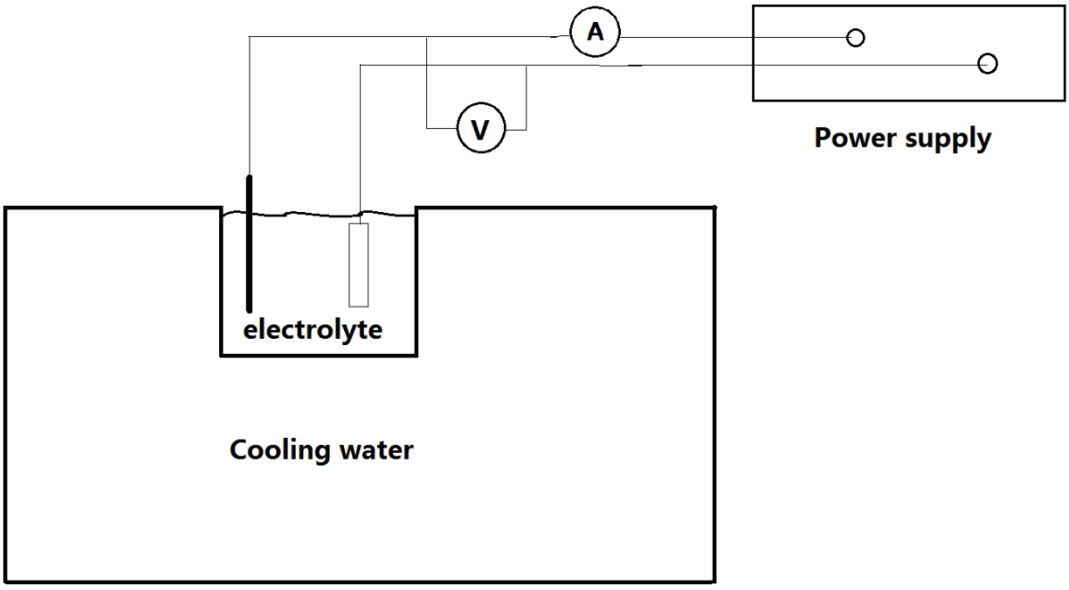

Figure 2.1 Plasma electrolytic oxidation setup.

The voltage will be rapidly raised from 0V to 250V. Voltage rising will be stopped when it reaches critical point. A replenish for electrolyte will be carried out when the system is beyond critical point in order to keep a continuous result.

As the power supply increases its voltage output, the potential difference between anode and electrolyte increases along with it. The V-I relation is shown in Figure 2.2.

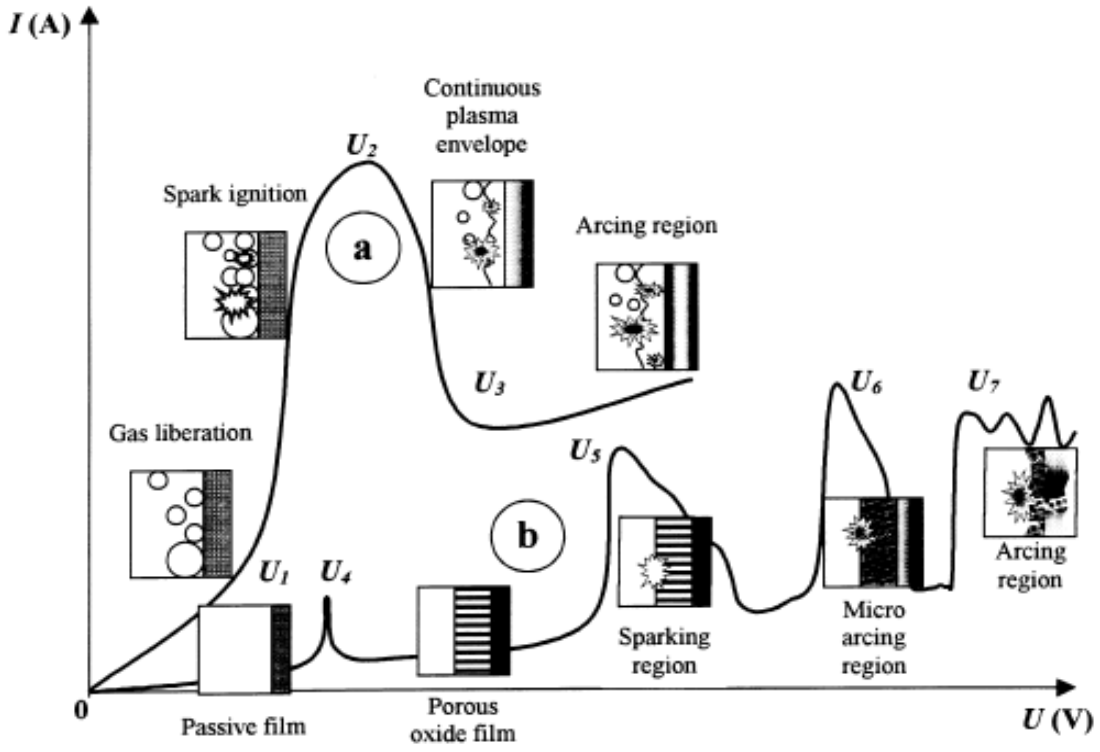

Figure 2.2 Schematic representation of plasma electrolytic oxidation.
Source: [13]

In the first stage, at low voltages, the electrochemical passivation takes place first. The metal substrate reacts with electrolyte and forms a passive film. In this stage, a common reaction of anodic polarization is taking place as normal passivation of metal. This stage is shown in Figure 2.2, U-I curve B.

In the second stage, at middle level voltages, a porous oxide layer continues to form from the original passive film by the electrical deposition effect. As the potential different between gas phase layer and metal surface will create a carrying current for ionized atom to be transferred to surface of metal, and a chemical-active net of porous oxide layer is formed by the ions that carried by the current. As the porous layer grows over the critical thickness, a breakdown of layer will take place. The dielectric film will break

through by the instable porous film for an ionized cloud which results from the peel off from porous film, will charge the dielectric film, and the cause a sparking for the conducting path is created. And such sparking will increase current density, peel off the porous film and leaves a rough surface of substrate.

In the final stage, when the voltage is above the critical point, the arcing stage takes place and a micro charge tunneling is formed to carry the ions to the surface of substrate and thus a layer of deposition is formed

The micro charge tunneling effect is shown in Figure 2.3.

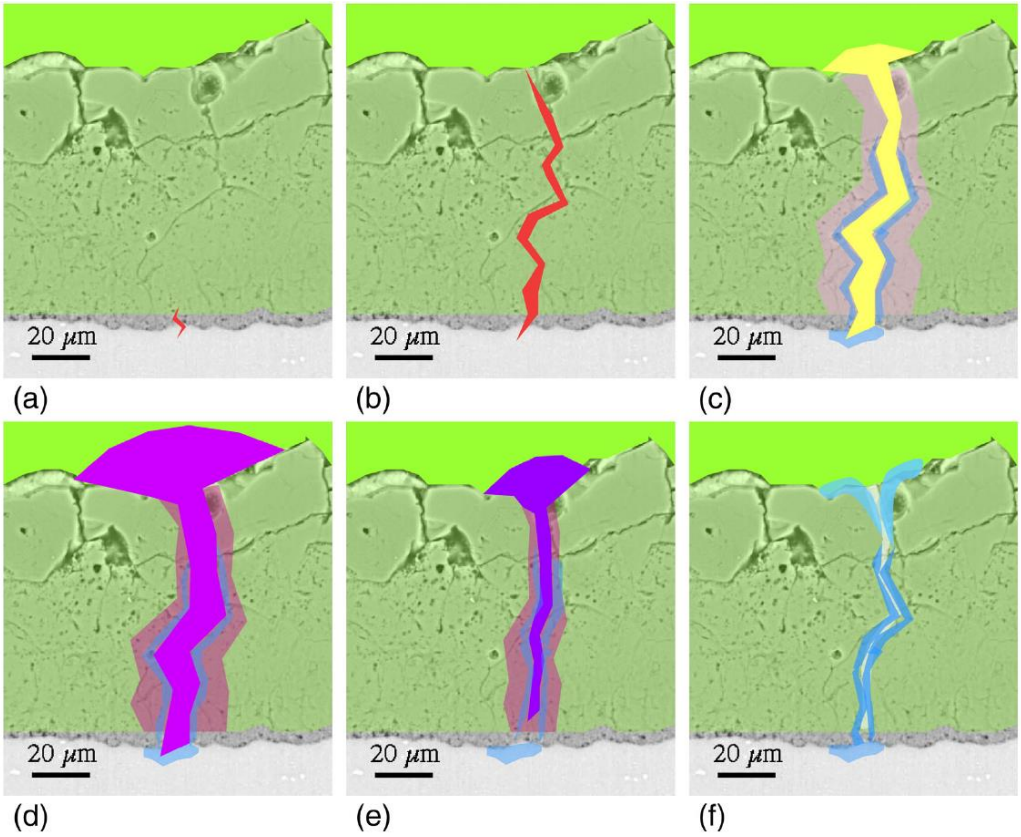

Figure 2.3 Schematic representation of plasma electrolytic oxidation discharge. (a) initial electrical breakdown, (b) development of the plasma channel through the coating thickness, (c) initial bubble growth and formation of oxide in the plasma, (d) bubble expansion and heating of region around discharge, (e) shrinkage and cooling as the plasma resistance rises, causing the current to fall, and (f) final quenching and expulsion of some liquefied oxide from the channel.

Source: [14]

In summary, the plasma electrolytic oxidation utilizes the micro discharge to transfer and deposit ionized atoms to the surface of substrate and forms a dense oxide layer.

There are two surface treatments for Titanium Grade 5: Plasma Electrolytic Oxidation of oxide layer and PEO deposition of HA.

The electrolyte used for oxide and HA coating are different, shown in Table 2.1. The ingredients will be explained in following paragraph.

Table 2.1 List of Electrolytes

Treatment	Composition	Concentration (mass fraction %)
Oxide coating	NaAlO	2%
	KH_2PO_4	5%
Hydroxyapatite coating	EDTA	1%
	KH_2PO_4	5%
	$Ca(OH)_2$	3%

2.2.1 Oxidation Layer Formation

The Titanium Grade 5 alloy will be treated by Plasma Electrolytic Oxidation to form an oxide layer. The ingredients for oxide coating are sodium aluminate and monopotassium phosphate. The electrolyte is buffered to pH of 11 to provide an alkaline environment. The alkaline environment enables the saturation of hydroxyl ions and creates a negative charged electrolyte -substrate interface on electrolyte film boiling side.

The sodium aluminate acts as the source of alumina and monopotassium phosphate as the oxidizing agent. As the voltage beyond critical point and the PEO process is in the final stage, the phosphate group will react with Titanium and generate negative charged

phosphate-titanium group on the surface of substrate; at the same time the sodium aluminate is ionized and Al-acid ions is freed to react with the active phosphate-titanium group. After the alumina binding with phosphate-titanium group, an amorphous layer will deposit onto the surface of substrate. As the alumina–phosphate group condensates, a porous structure is formed and attached to the Titanium substrate [15].

In the aqua environment, there is only local temperature increasing, but the global temperature is in cold stage. During the sparking stage, the temperature increases up to 1500 K, and all ions are ionized to plasma stage. As the elements are bond to the sample, its temperature drop to cold stage and settle down the matrix of coating. The fast cooling effect will reduce the thermal expansion dislocation and cracks, for the coating during thermal spray process and results in high temperature deposition. The thermal spray coating layer often undergoes at 1500 K when deposition forms. As the coating layer cools down, the volume change is relatively great for the significant change in temperature [15][16][17].

In general, an intense reaction occurs at the surface of metal plate. The electrolyte attacks the metal surface and the react with metal, forming a dense and thick ceramic layer[18].

2.2.2 Deposition of HA

As same setup of oxide process, the power supply will create an electrical potential different between electrolyte and metal plate. The ingredients of electrolyte are Edetic Acid (EDTA), Monopotassium phosphate and Calcium hydroxide. Monopotassium phosphate is the oxidation agent and substrate of HA. Calcium hydroxide is the source of

Calcium in HA, and it's also the pH buffer to provide an alkaline environment. EDTA is the chelating agent which will enrich Calcium ions in solution by preventing deposition. Moreover, the Calcium salt of EDTA is negative charged, making it able to move to the cathode part of solution, i.e. metal substrate [18].

At first, when at the low voltage, the oxide layer is to be formed continually. As a result of electrochemical passive process a passive layer will be forming on the surface of Titanium substrate. With the increasing of voltage, the negative charged hydroxyl ion begins to bind to the Titanium in active state. Then the bonding between hydrogen and oxygen is broken by the discharge of micro-arc initiated by discharge in dielectric layer. The oxygen which is bonding to Titanium passive layer is left positive charged, and the phosphate group will be binding to the positive charged oxygen. Once the bonding is completed, a net of oxygen- phosphate is formed and the Calcium ions are binding to available positions left on phosphate base. Thus a HA coating is completed by a plasma-chemical process. The chemical nature of HA forming is shown [18]:

$$Ca^{2+} + PO_4^{3-} + OH^- = Ca_5(PO_4)_3(OH) \qquad (2.1)$$

In general, after a passive layer is formed on the surface of substrate, the electrolyte will react with the surface of the oxide layer and forming a hydroxyapatite layer, shown in Figure 2.4.

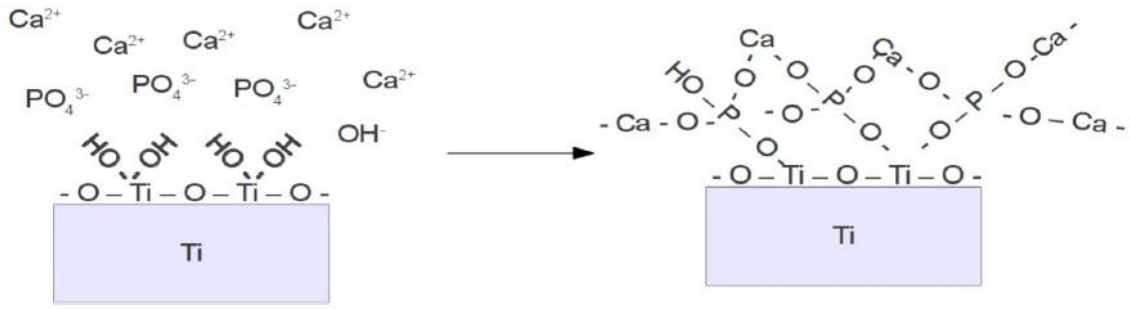

Figure 2.4 Schematic representation of forming HA coating.
Source: [19]

CHAPTER 3

SURFACE MORPHOLGY

The surface morphology is important to the performance of bio-material and the evaluation of surface coating [20][21]. The surface morphology is characterized by Optical Microscope and Scanning Electron Microscope.

3.1 Optical Microscope

There are two surface treatments for Titanium Grade 5: Plasma Electrolytic Oxidation of oxide layer and PEO deposition of HA. Both samples are cleaned in alcohol in ultrasound tank and dried by compress air. Then the samples are examined by an Optical Microscope Zeiss HD 100.

3.1.1 PEO Treated Ti-6Al-4V Sample With Oxide Coating, Surface

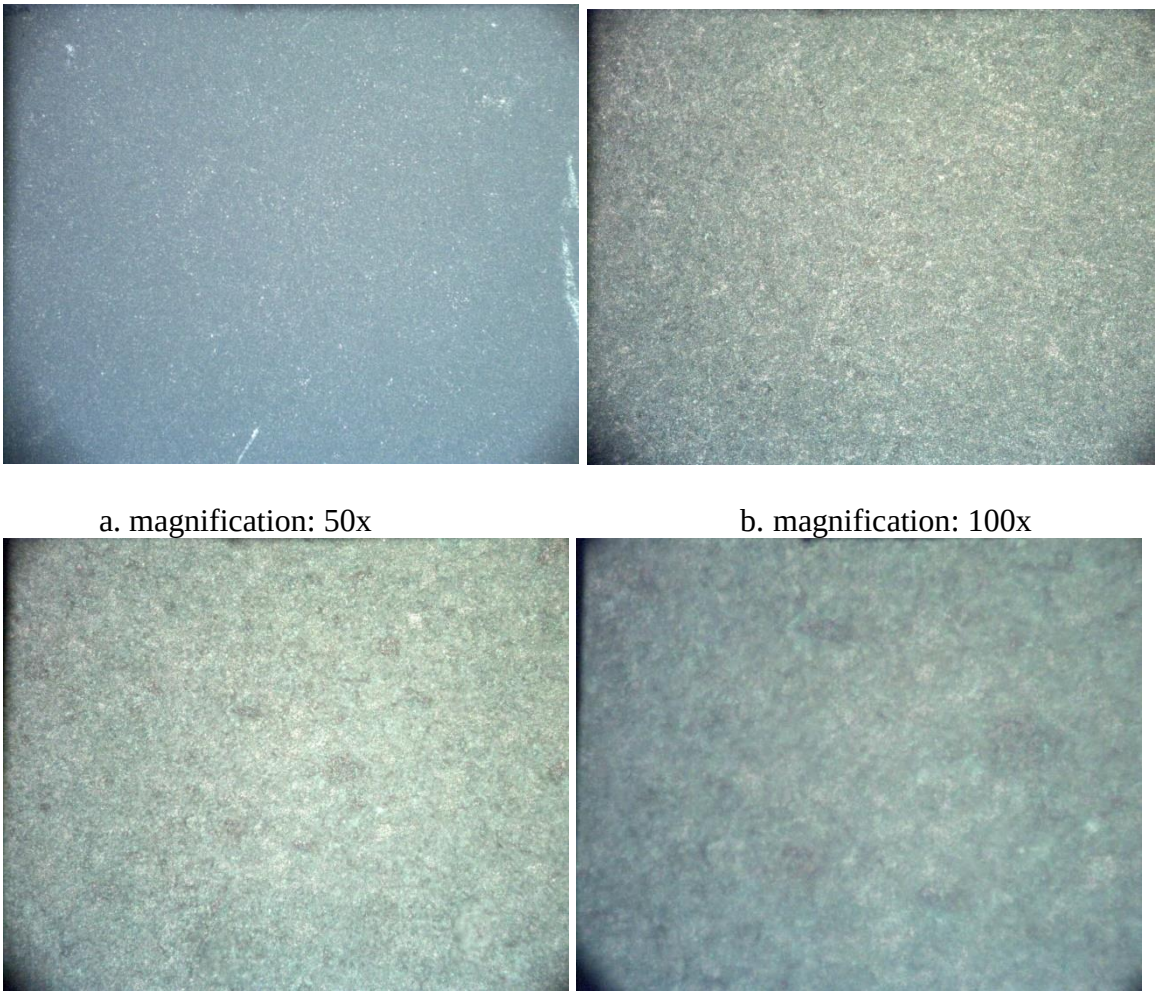

a. magnification: 50x b. magnification: 100x

c. magnification: 500x d. magnification: 1000x

Figure 3.1 Optical images of PEO treated sample with oxide coating, surface optical image.

The high light reflection in this view is the metallic reflection from the substrate, which indicates a peel-off of coating, a defect during process, or an uneven coating. In the low magnification, 50x and 200x, the surface of samples shows a dense layer of ceramic structure. The oxide layer is uniform throughout the surface of coating. The surface consists of aluminum oxide ceramic which firmly formed to the substrate. And there are no high light reflections that can be found in this view.

In high magnification, 500x and 1000x, the coating shows a drape landscape. This

is defined by the chemical nature of the coating. The coating is ceramic in structure and unpolished thus result the random reflections in the view which is the uneven surface of aluminum oxide coating [22].

3.1.2 PEO Treated Sample With Oxide Coating, Cross Section

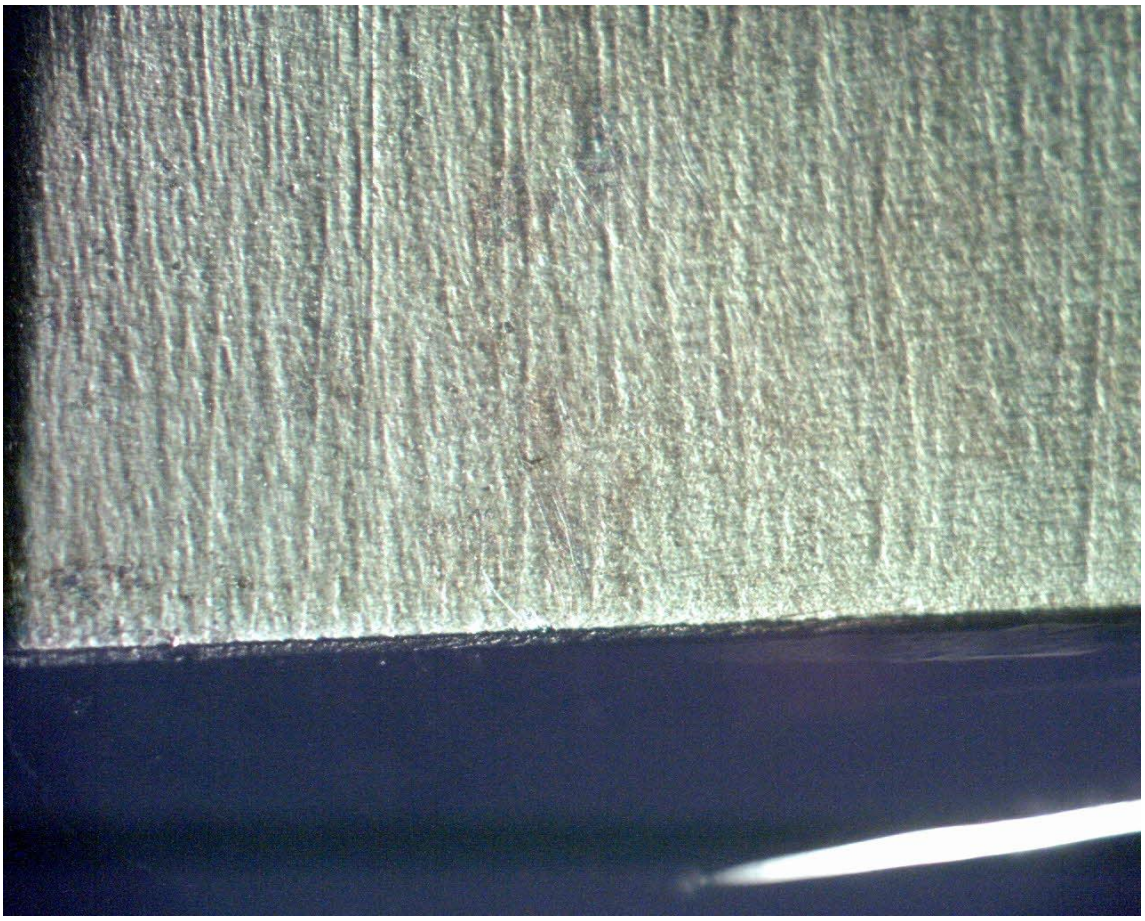

Figure 3.2 Optical image of cross-sectioned Ti-6Al-4V PEO treated sample, 50x.

Figure 3.3 Optical image of cross-sectioned Ti-6Al-4V PEO treated sample,100x.

In the Figure 3.2 and Figure 3.3, the cross section is free of erosion and blasting of PEO process.

3.1.3 PEO Treated Sample With HA Coating, Surface

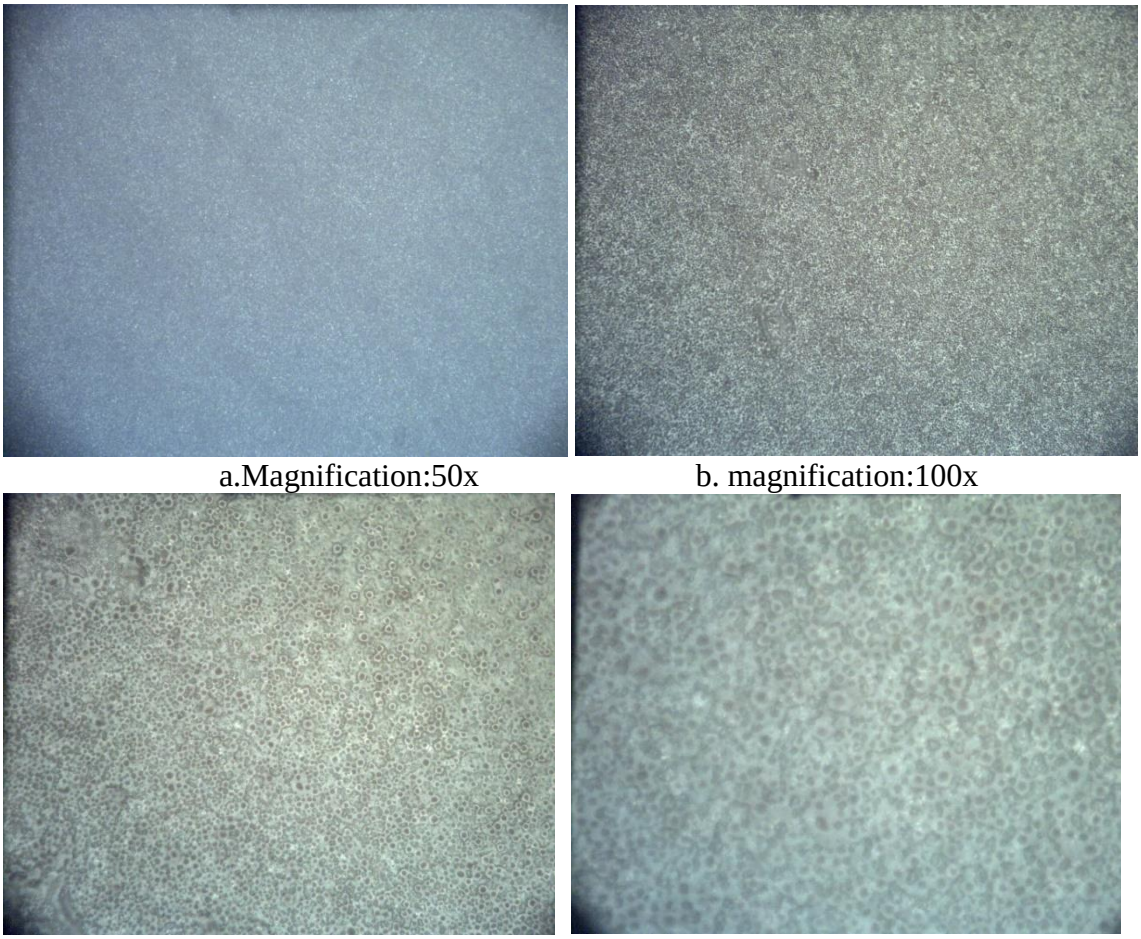

a.Magnification:50x b. magnification:100x

c. Magnification: 500x d. Magnification:1000x

Figure 3.4 Optical images PEO treated samples with HA coating.

The HA coated surface is analyzed by optical microscope with magnification of 50x, 100x, 500x and 1000x. In low magnification, 50x and 100x, the surface of sample is dusky and dim, under the condition of uniform and thick coating of HA.

In high magnification, the HA coating has a porous structure with a honeycomb net topography. Such structure is the result of crystal forming of HA[23].

As the PEO process depositing calcium and phosphorus onto the Titanium, the Ti-Ca-P-O reaction takes place first and creating a calcium titanate phase closing to titanium substrate [24]. The calcium titanate structure is similar with coating on the oxide coating sample on the last part; it has a porous structure which is able to bond to HA. Then

the HA forming reaction take place and a layer of HA is forming on top of calcium titanate layer. As the elements on metal- electrolyte interface saturated, the crystal forms as the local temperature drops to cold stage and leaves the porous-honeycomb net topography set [25][26].

This porous structure enable bone precursor cell, myoblast affinity to the implant of such coating, thus gives a great tissue-implant connection.

3.1.4 Cross Section of PEO Treated Samples with HA Coating, Cross Section

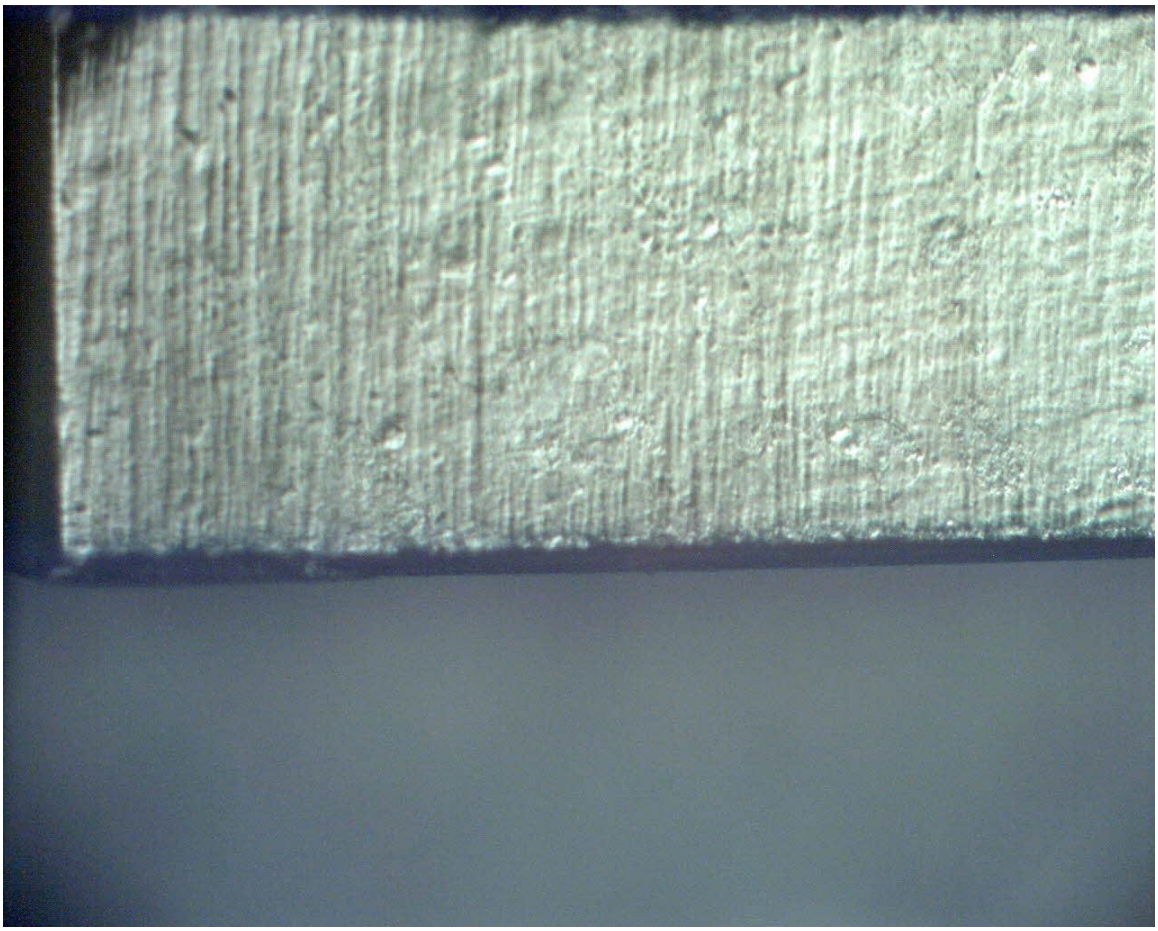

Figure 3.5 PEO treated sample with HA coating, cross section optical image, magnification: 50x.

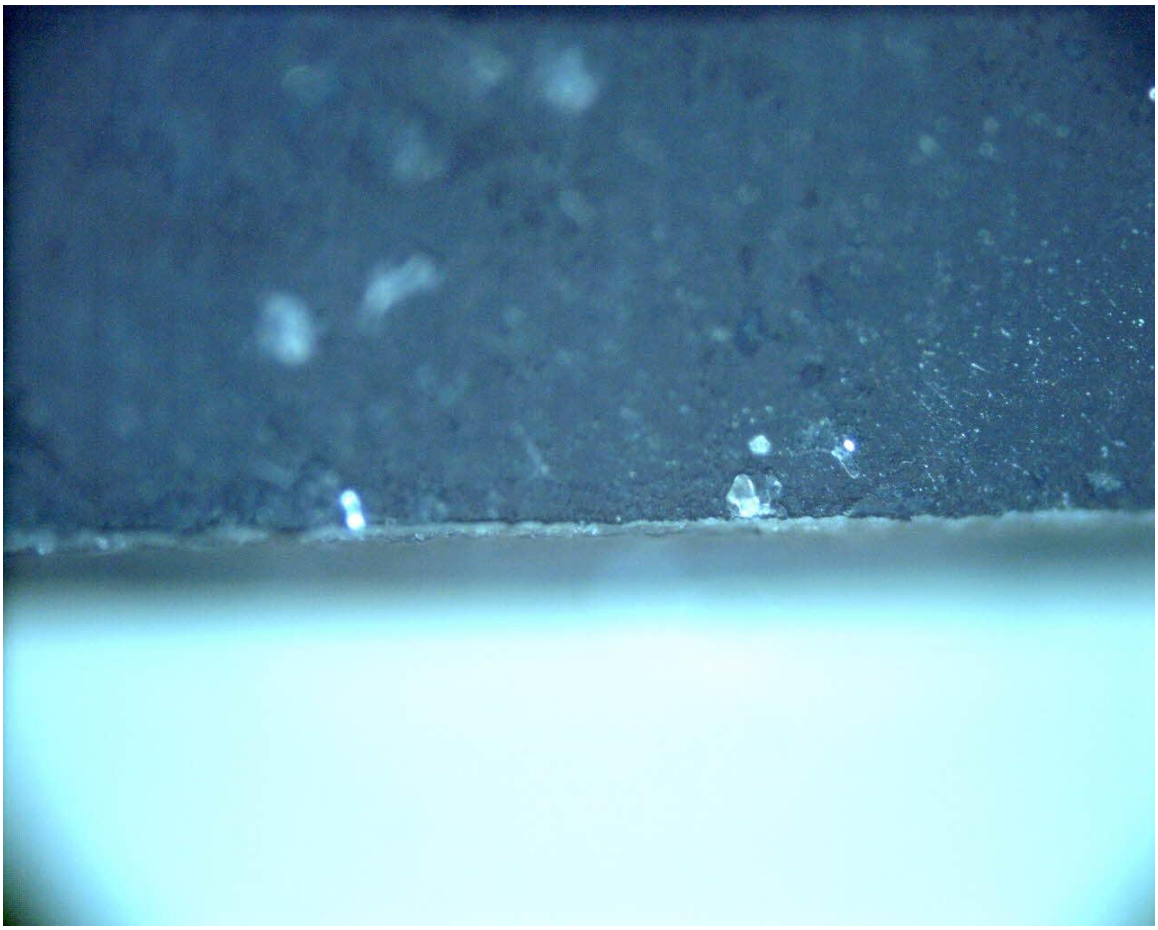

Figure 3.6 Optical image of PEO treated sample with HA coating, 100x.

In previous experiments there are samples which its surfaces had been damage by arcing of bubble blasting. In the failed experiment, the cross section shows discontinuous line on surface and blast pit on and below coating. Such failure results in coating peel off and defects in coating.

In this cross section image of HA sample, the HA coating layer is formed on the surface of substrate in continuous line without defects or blasting pit. Furthermore there are no sign of erosion or bomb blast of bubble which will create a local curve coating. The coating intersection is aligning with the original substrate surface [27].

3.2 Scanning Electron Microscope

There are two surface treatments for Titanium Grade 5: Plasma Electrolytic Oxidation of oxide layer and PEO deposition of HA samples were be analyzed by SEM. Also the elements distribution is carried out by Energy Dispersive Spectroscopy (EDS).

3.2.1 PEO Treated Sample With Oxide Coating

SEM results from the oxide coating samples are is shown in Figure 3.2.1.1.

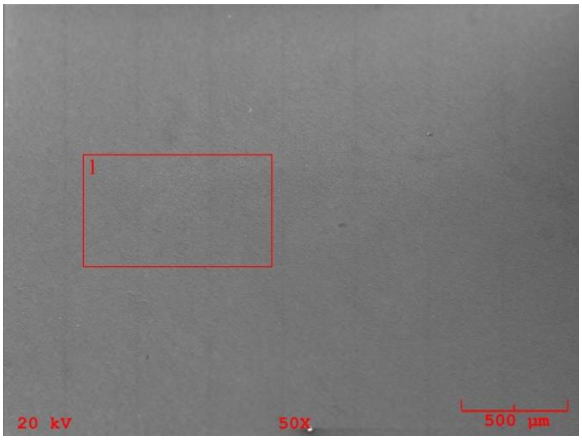

a. Magnification:50x

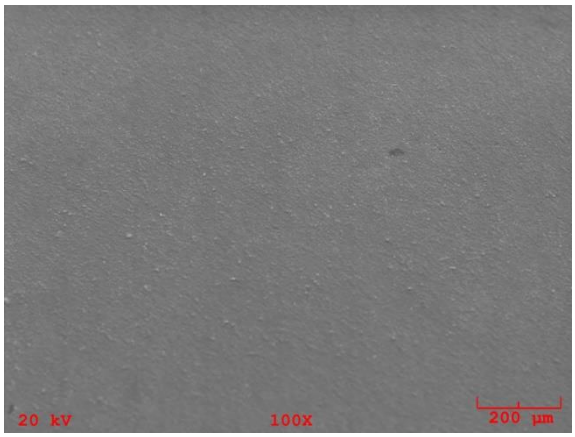

b. Magnification:100x

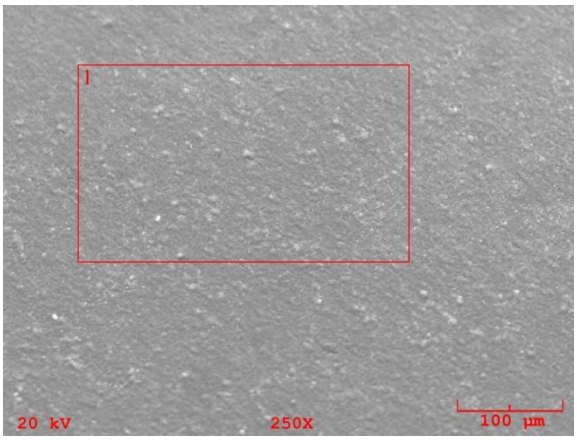

c.Magnification:250x

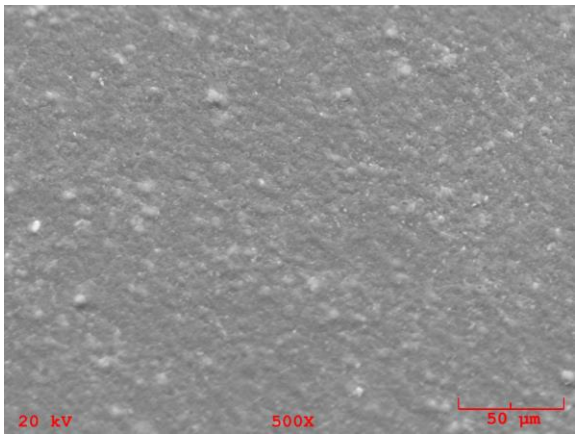

d. Magnification: 500x

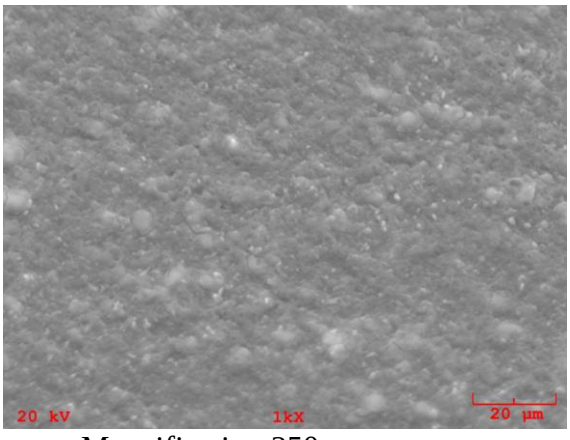

e.Magnification:250x

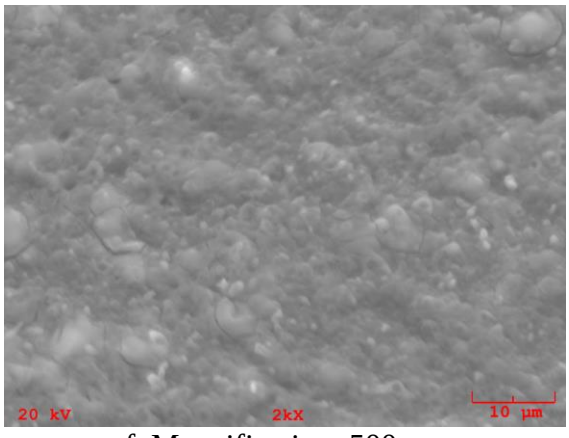

f. Magnification: 500x

Figure 3.7 SEM images of PEO treated samples with oxide coating.

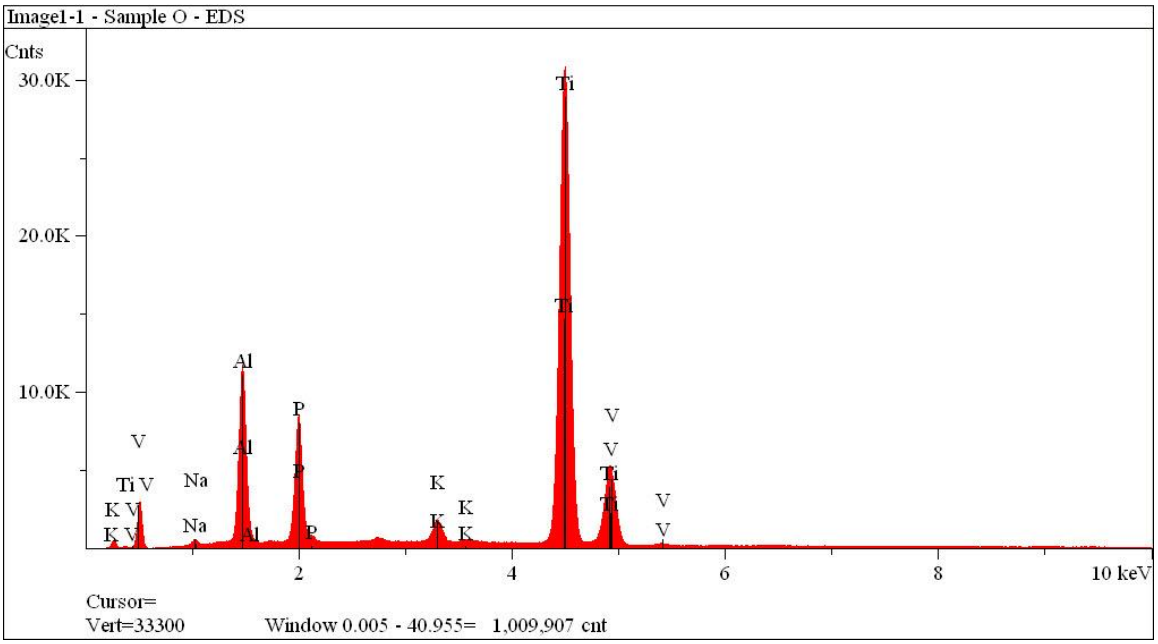

Figure 3.8 EDS data in SEM image a. area 1.

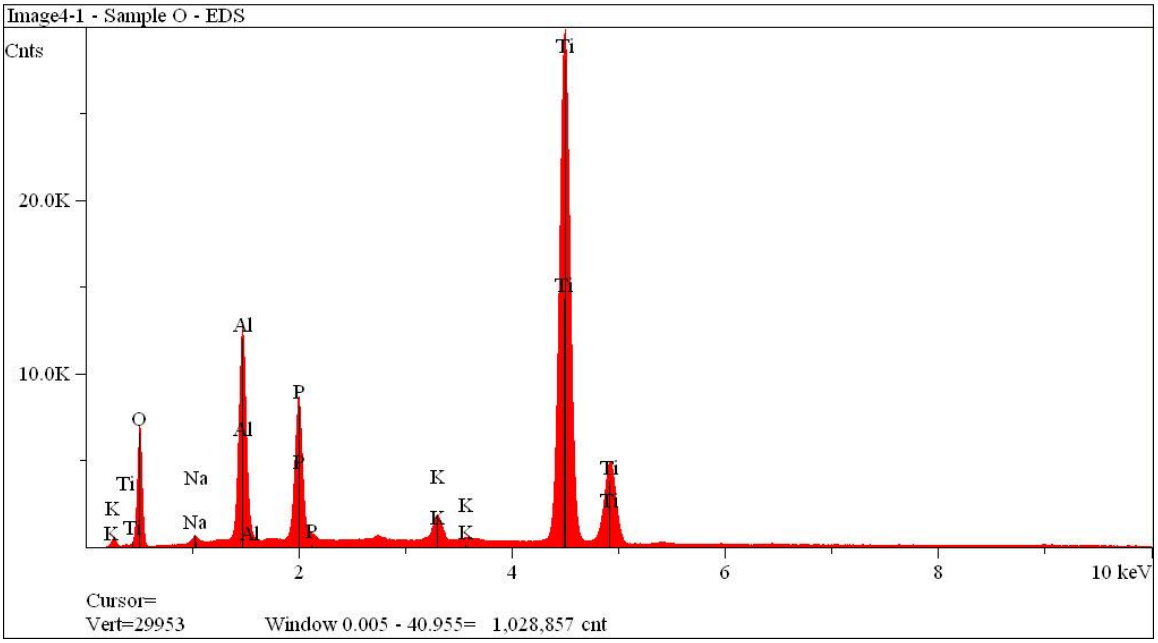

Figure 3.9 EDS data in SEM image c. area 1.

The EDS data in 50x and 250x on surface of samples are shown in Figure 3.8 and Figure 3.9. Except the Titanium counts from the substrate, there are three major counts of elements which can be found: aluminum, phosphate, and oxygen. These three elements are

evidence of successful coating. [28] [29]

3.2.2 PEO Treated Sample With HA Coating

The HA coated sample is shown in Figure 3.10.

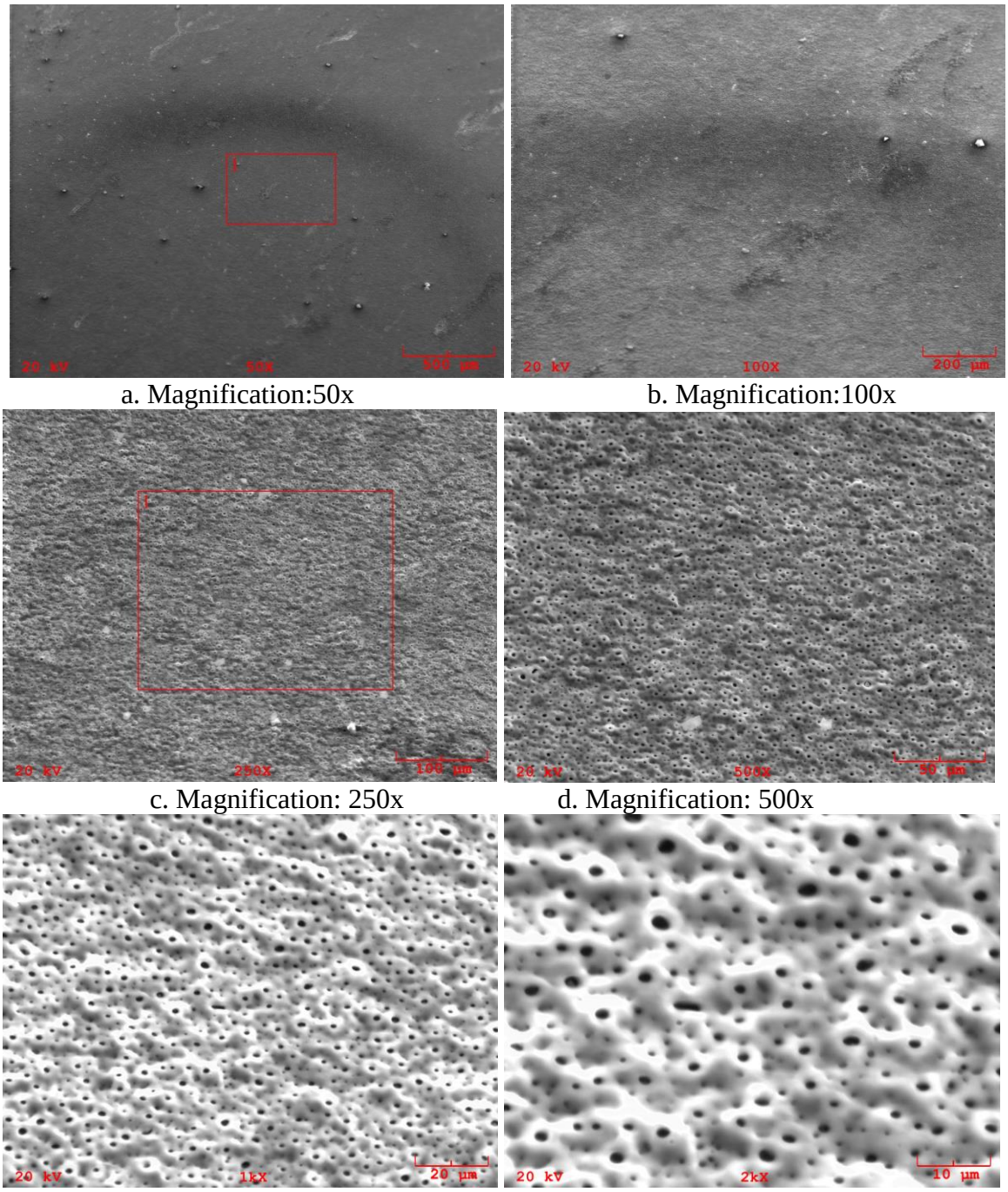

a. Magnification:50x b. Magnification:100x

c. Magnification: 250x d. Magnification: 500x

e.Magnification:1000x f. Magnification: 2000x

Figure 3.10 SEM images of PEO treated sample with HA coating.

In the low magnification of SEM images, 50x and 100x, a flat coating surface is formed on the substrate. Also, the surface shows no high light area, which means there are no defects or peel off that will cause reflection in both magnifications.

In the higher magnification of SEM images, 250x and 500x, a uniform but coarse surface is observed. As the magnification increases, a flat surface in low magnification emerge its fine structure: coarse and porous network ceramic dense layer. Moreover the ceramic layer in this magnification shows consistency in pattern, which means the coating, has formed under similar condition which means no other side effect process takes place which would create uneven coating surface.

At the highest magnification of SEM images, 1000x and 2000x, a honeycomb network can be observed. The porous honeycomb is the typically HA crystal morphology, as the interconnected net grow in both parallel surface and perpendicular to the surface as it has been discussed in Chapter 3. The thee-dimensional growing creates an ant nest HA scaffold which is on the top of substrate. The bone affinity will benefit from the porous layer for it fits the requirement for bone affinity. The average porous diameter is around 1μm [30].

The EDS data of HA coated sample in 50x and 250x area is shown Figure 3.11 and Figure 3.12

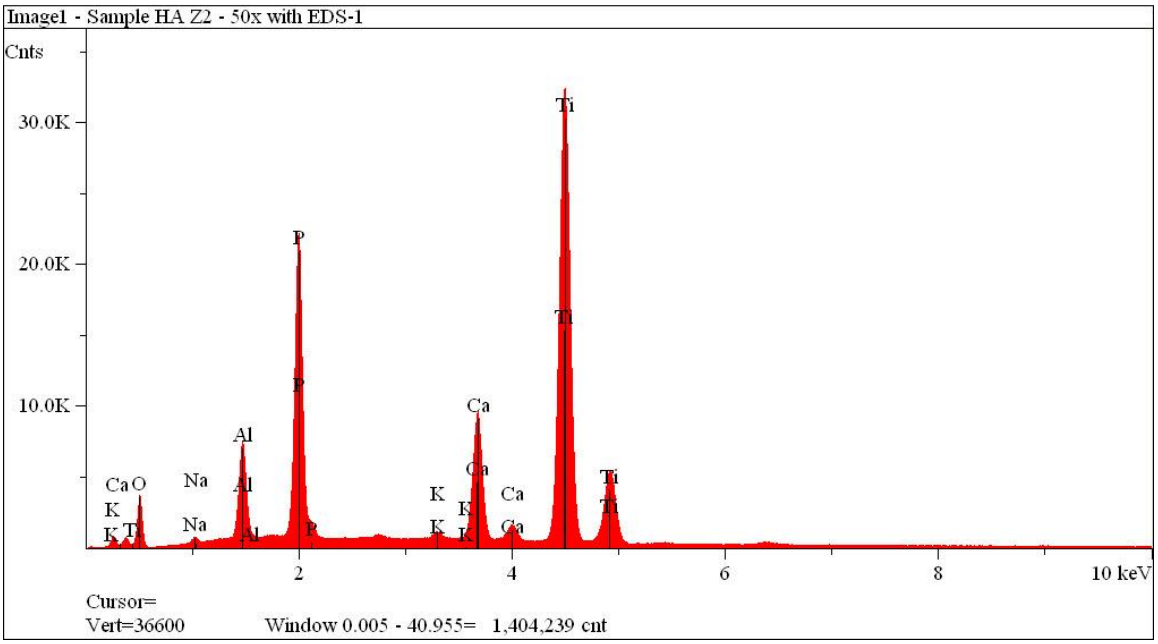

Figure 3.11 EDS data in SEM image a. area 1.

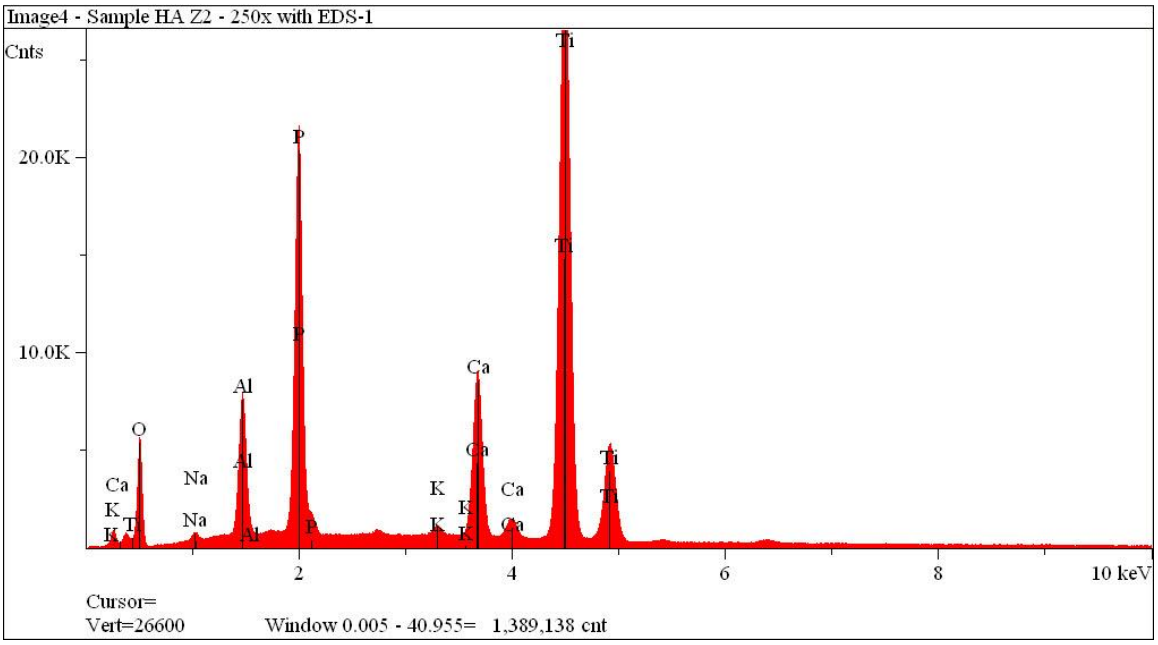

Figure 3.12 EDS data in SEM image C. area 1.

In the EDS data, there are five significant peaks: O, Al, P, Ca, Ti. As there are significant amount of Ti in substrate, the Ti peaks has the maximum counts. There are also significant peaks of P and O indicating the phosphate group existence. Also there are Ca counts can be found, as the cation of HA chemical component .The counts of Ca is not as

high as it should be, for there abundant area of Ca is at 60 μm distance from the surface of top of the coating, as it has been discussed in elemental distribution part of Chapter 3. [31]

CHAPTER 4

X-RAY DIFFARCTION

The crystallography will be discussed in this chapter. The X-ray diffraction is one of common analyzing method of crystallography. When the incoming X-rays hit the material, the rays will be scattered by the high density crystal plane. As the diffraction ray is received, a pattern will be drawn by the result of diffraction signal. The different structure and phase can be identified by the peaks of diffraction pattern. The oxide and HA coated samples are analyzed at Advanced Photon Source at the Argonne National Laboratory.

4.1 The Advanced Photon Source

The source of X-ray is provided by The Advanced Photon Source from Argonne National Laboratory. The high power energy beam is exported from synchrotron radiation storage ring by the synchrotron radiation. As the beam is selected out, the light is tailored and focused to preform X-ray diffraction.

The high energy of beam makes it possible for the light to focus in a circle of diameter of 0.2 μm. The wavelength of X-ray is 0.61992 Å and the energy of light is 20 keV. The sample is cut to show it cross section to review the structure.

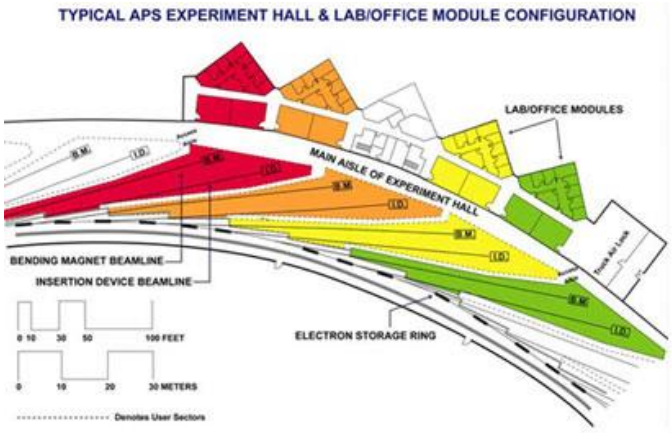

Figure 3.1 Experiment hall setup of APS at the ANL.
Source: http://www.anl.gov/

4.2 X-ray diffraction

There are two surface treatments for Titanium Grade 5: Plasma Electrolytic Oxidation of oxide layer and PEO deposition of HA. The scanning is carried out by increment step of 0.5 micrometers

4.2.1 PEO Oxidized Samples

An XRD is taken at the 16th step from the coating surface. It's estimated to be the center of the coating and its 8 micrometers from the surface of coating. The data is shown in Figure 3.2.

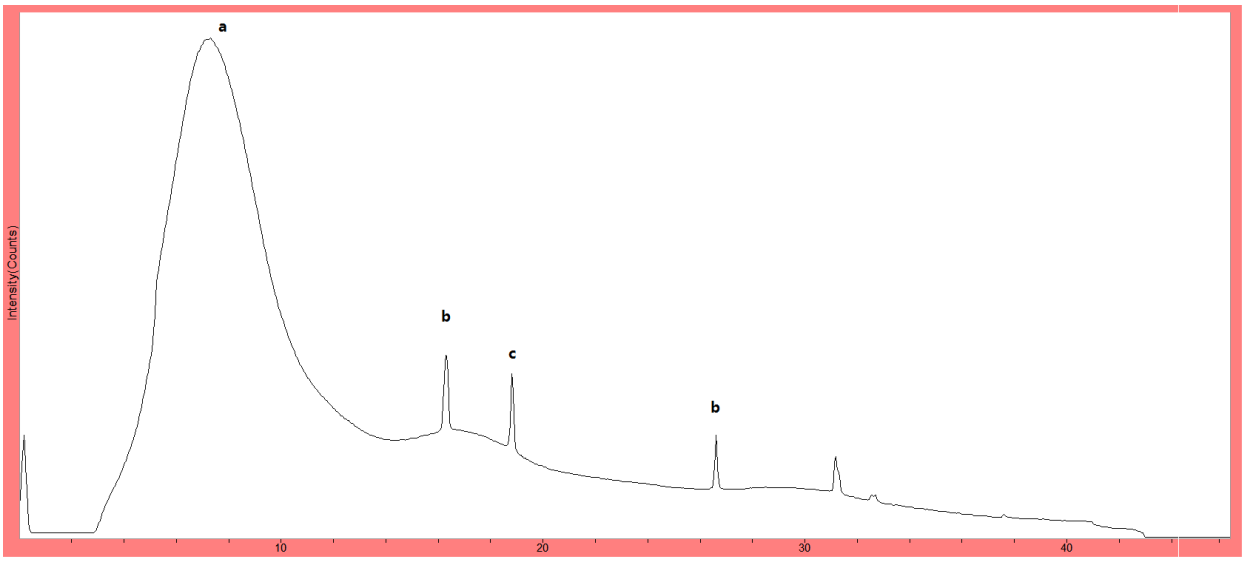

Figure 3.2 XRD diffraction of samples with oxidized sample. a:amorphous peak; b:Titanium.c: Al.

At the low diffraction angle, there is an amorphous peak found. Such an amorphous peak is the result of PEO treated sample with oxide coating. The PEO treated sample with oxide coating consists of ceramic structure which has less or no crystal structure at all. The intensity of amorphous is at high level compared with other peaks. That is to say the amorphous consist of major micro-structure in this cross section area.

4.2.2 HA Coated Samples

The XRD diffraction is shown in Figure 3.3, the data is collected from the 84th step of scanning, 42 micrometers from surface.

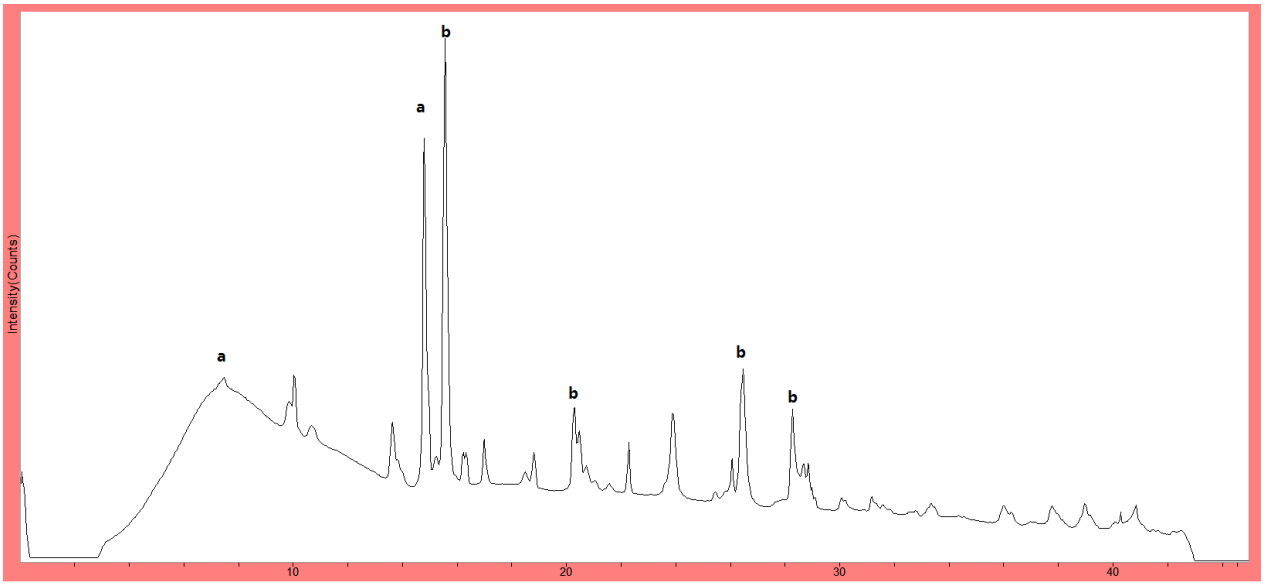

Figure 3.3 XRD diffraction of sample with HA coating. a: HA; b: Titanium.

In the XRD data, the peaks of HA can be found. There is a peak which is almost covered by the amorphous peak. But the second peak of HA has a high count. The crystal HA is crucial to the bone affinity, and in the center of coating cross section area the peak of crystal HA can be found, indicating it's suitable for bio-material coating. [32]

4.3 Elements Distribution

The elements distribution is analyzed by X-ray Fluorescence Spectrometer at the ANL.

4.3.1 HA Coated Samples

The elemental distribution of HA coated sample is shown in Figure 3.4.

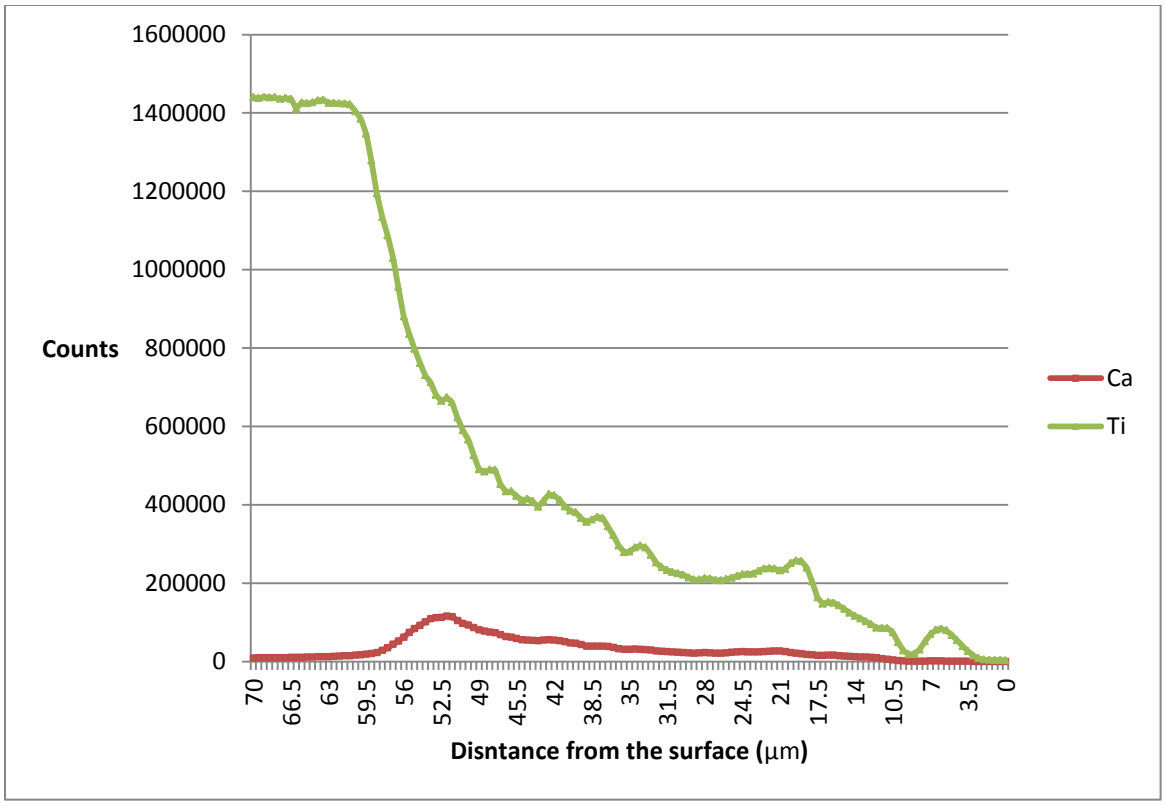

Figure 3.4 Elements distribution in HA coating sample.

There are two lines representing two elements: red line for Calcium, green line for Titanium.

As for Titanium, the Titanium counts which represents the content distribution of Titanium, are gradually increased from the surface of the sample and reached maximum threshold at 60 µm. Such a length is estimated length from the top of coating to the Titanium substrate.

However, the peaks between 0µm to 60µm show there are mixture of Titanium with Calcium structure in the coating area.

The Calcium counts which represents the content distribution of Calcium, is gradually increased from the 0 µm, and it reaches peak at 52 µm from the top of the coating. As the Ca is the cation of HA, the counts can identify abundant level of the coating layer.

With the Titanium counts reach maximum and the Ca line touches the zero line, the coating ends at 60 μm from surface of coating.

CHAPTER 5

ELECTROCHEMICAL TEST

Corrosion is a reaction between environment and metal. In order to analyze the samples in vitro electrochemical behavior, a list of electrochemical tests is carried out, shown in Table 5.1.

5.1 Test of Samples

The list of samples and test method is shown in Table 5.1.

Table 5.1 List of Samples and Test Method

Samples	Test Method
Titanium Grade 5(Ti-6Al-4V)	Tafel
Titanium Grade 2	Tafel
Titanium Grade 5(Ti-6Al-4V) with oxide coating	Tafel, EIS
Titanium Grade 5 (Ti-6Al-4V)with HA coating	Tafel, EIS

5.2 Potential Dynamic

5.2.1 Plain Titanium Alloy Ti-6Al-4V

The Tafel plot is shown in Figure 5.1.

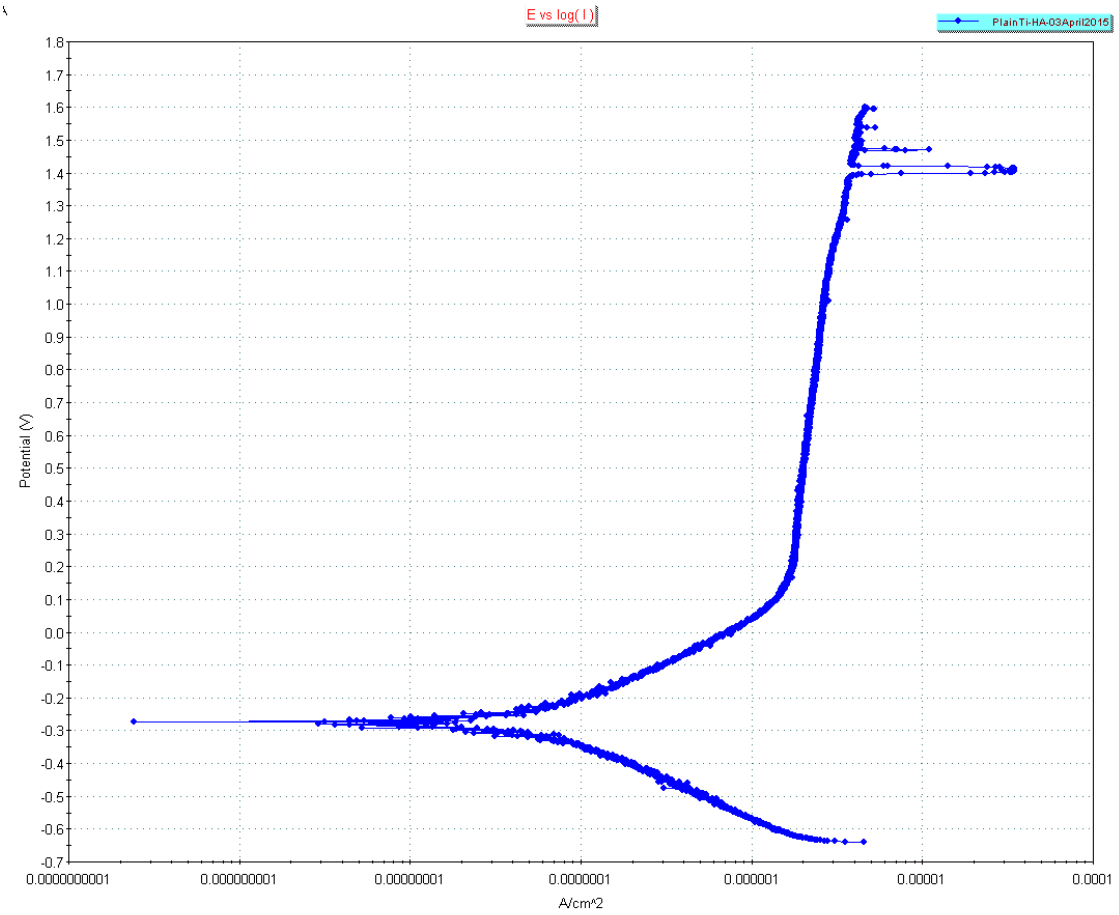

Figure 5.1 Potential dynamic plot of plain Titanium alloy Ti-6Al-4V.

In the Tafel region, the low voltages region, the electrochemical potential of plain alloy shows a typical behavior: from cathodic to anodic polarization.

As the potential difference which applied on the sample increases, the cathodic polarization takes place first, the concentration polarization controls at this stage. After the concentration polarization the active polarization is rate-controlling. With the current of cathodic and anodic polarization equal, the current drops at the minimum point. After the equal point, the anodic polarization takes the controlling place and the current gradually increases.

As the voltages increases above the Tafel region, the current is not increased along

with the voltage. Such behavior shows the uncoated Titanium Grade 5 is able to passive itself after the cathodic polarization. [33]

In the anodic polarization area, where the voltage is around 1.4 V, there are several abrupt currents boost. This oscillation results from a transformation from mass transport limited dissolution to passivity. Such breakdown indicates metastable in pitting. And it is easy infer that there is a stable pitting stage after the metastable pitting stage. The pitting surface can be found in the optical microscope image after the potential dynamic test is completed as shown in Figure 5.2.

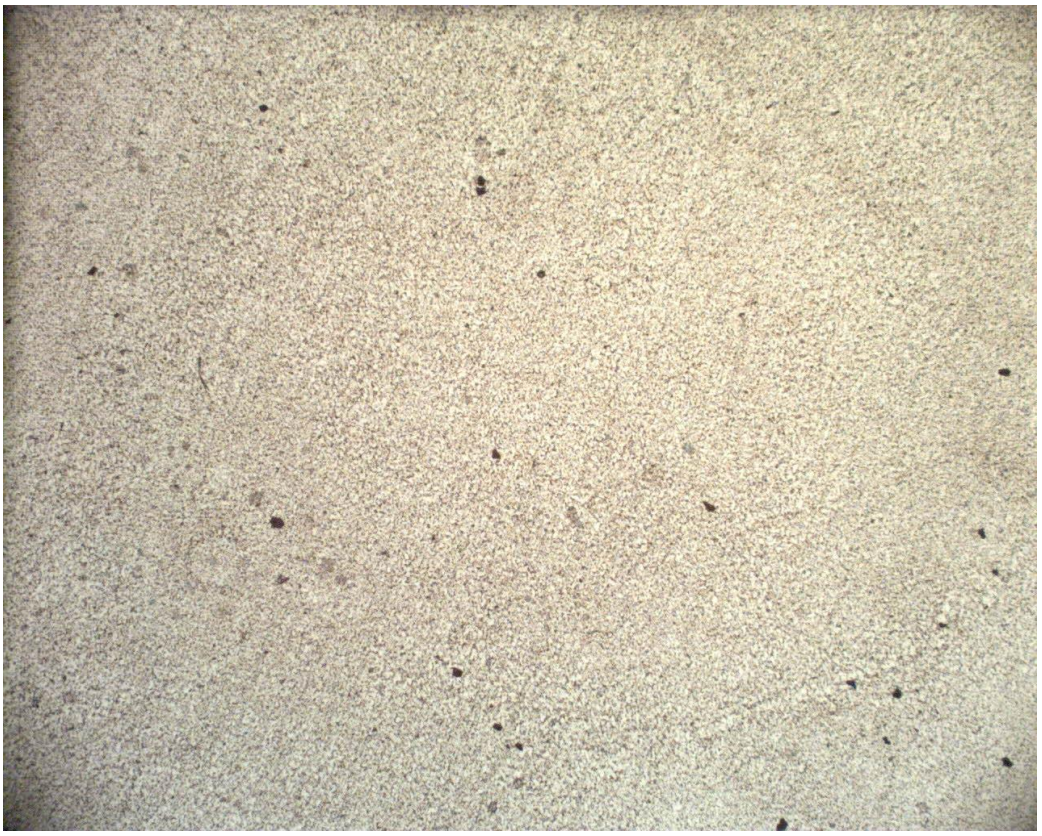

Figure 5.2 Pitting corrosion surface on Titanium alloy Ti-6Al-4V, magnification: 50x.

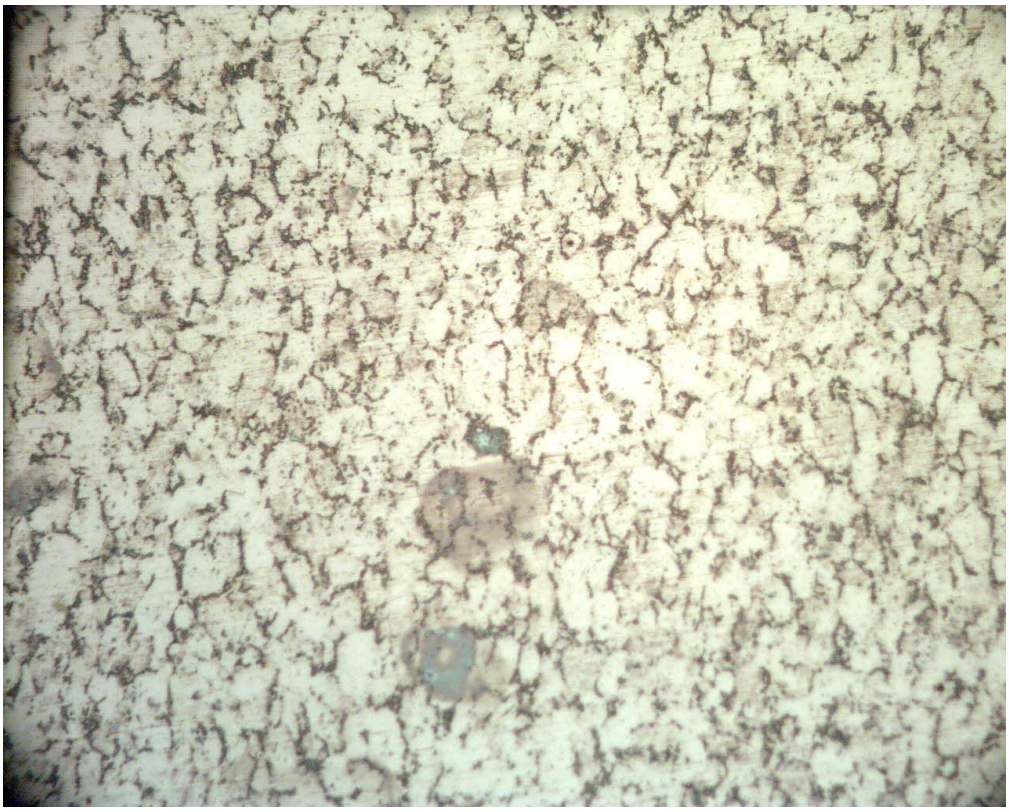

Figure 5.3 Pitting corrosion surface on Titanium alloy Ti-6Al-4V, magnification: 500x.

As shown in Figure 5.3, the dark points in magnification of 50x are the result of pitting corrosion. As the unprotected substrate is exposed to the corroding environment, the electrolyte attacks the curving surface and creates a high concentration area of ions [34]. With corroding taking place, the digging of corroding effect will create a pit as shown in the Figure 5.3. The close view of a single corrosion pit is shown at magnification of 500x, in Figure 5.4; it shows the digging takes place on a curving area [5][6].

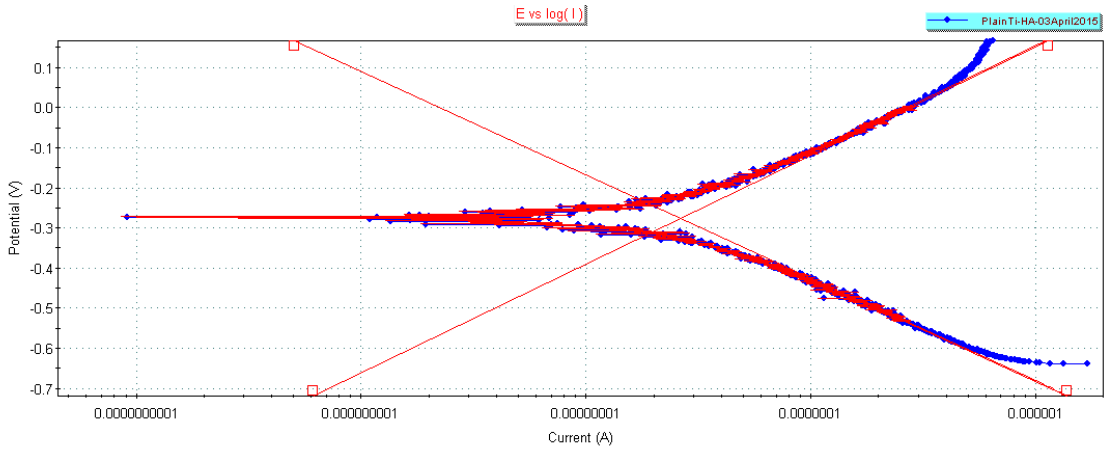

Figure 5.4 Tafel fit plot of plain Titanium alloy Ti-6Al-4V.

5.2.2 Plain Titanium Grade 2

The potential dynamic graph is shown in the Figure 5.5.

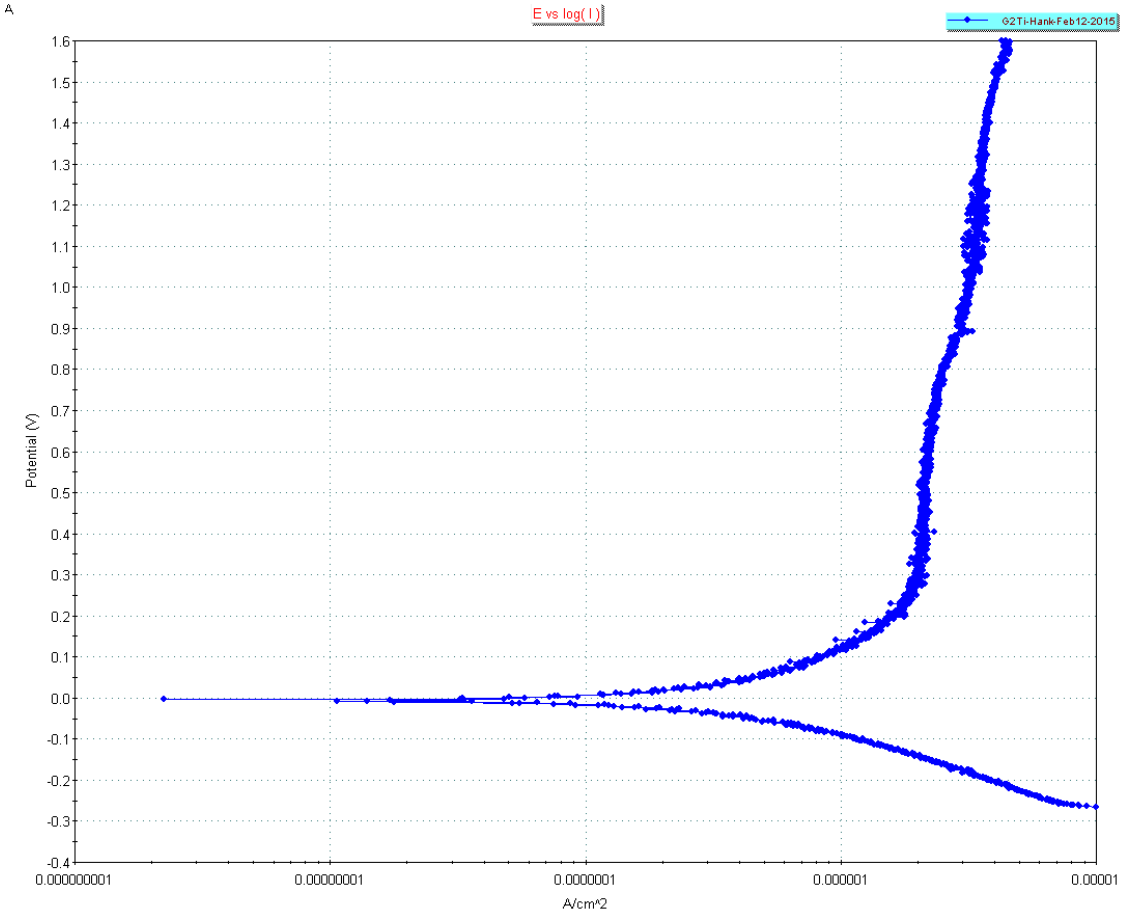

Figure 5.5 Potential dynamic graph of plain Titanium Grade 2.

A typical Tafel plot can be observed in the potential dynamic plot. The corrosion potential of this sample is much higher than the Grade 5 sample for the Grade 2 is pure metal, thus the metal can benefit from the absent of alloying elements and no micro local cell forms.[35]

At and above 0.9 V, the I-V curve shows a metastable oscillation which is a similar cause of Titanium Grade 5: the pitting corrosion. However, the pitting is not as severe as the Titanium Grade 5 sample. For the Titanium Grade 2 pure metal with no alloy element, the pitting effect is prohibit by absent of electrochemical cell [5][6].

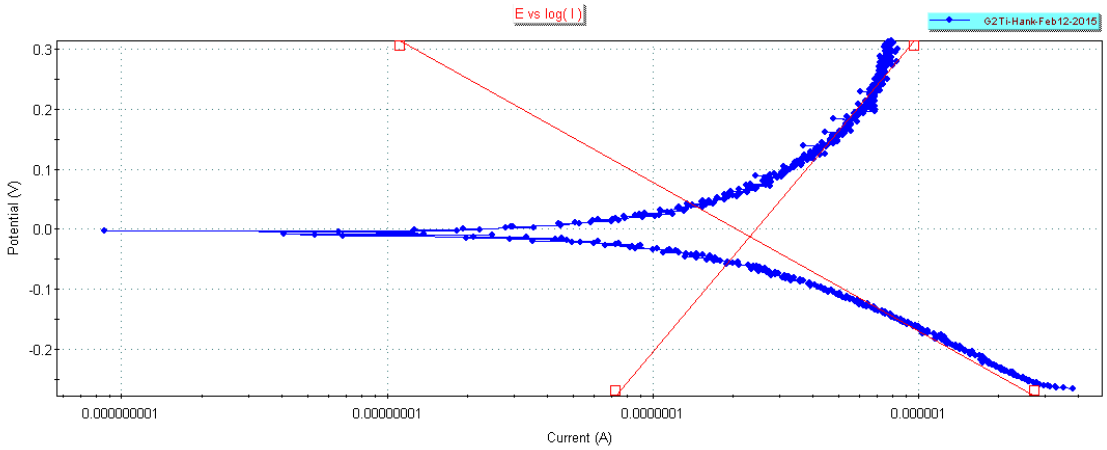

Figure 5.6 Tafel fit plot of plain Titanium Grade 2.

5.2.3 PEO treated sample with oxide coating of Titanium alloy-Ti-6Al-4V

The potential dynamic plot is shown in Figure 5.7.

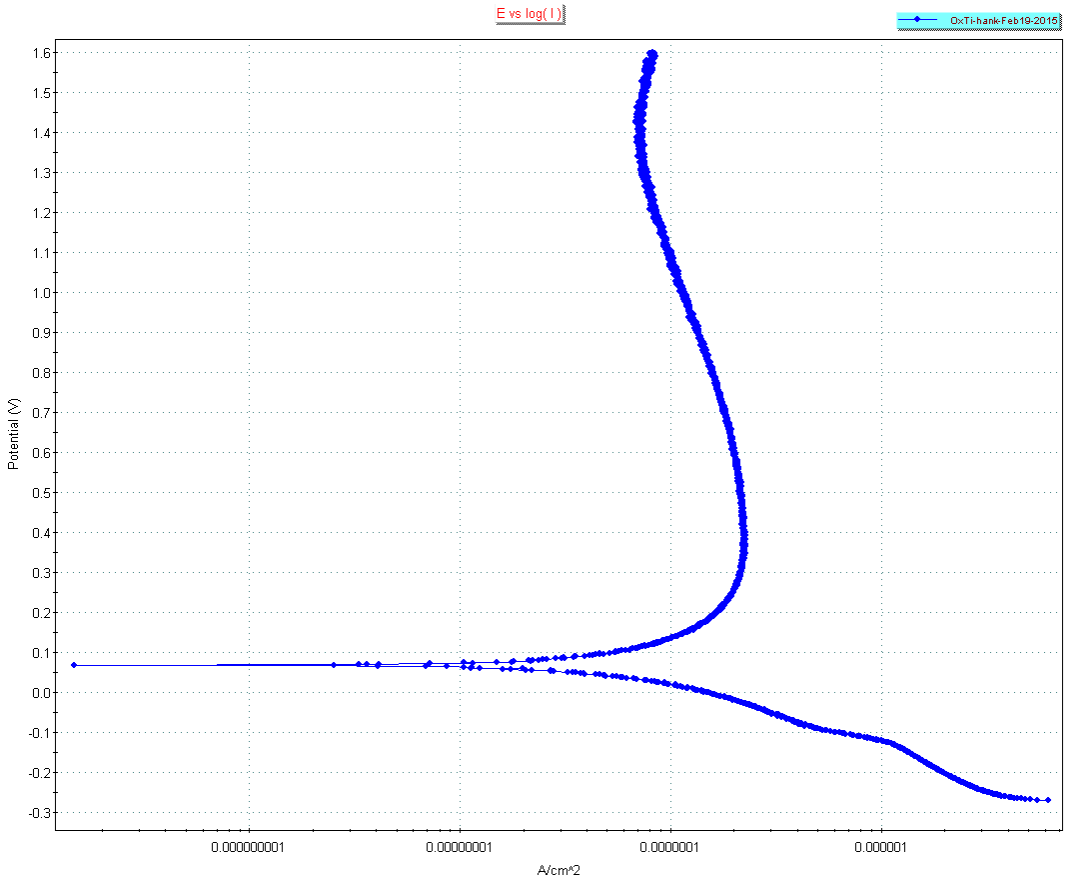

Figure 5.7 Potential dynamic plot of PEO treated sample with oxide coating on Titanium alloy Ti-6Al-4V.

As for cathodic to anodic polarization, the potential dynamic plot of oxidation sample shows a typical Tafel behavior, with a smooth polarization curve.

After the Tafel region, the slope of I-V curve is negative, in which the current decreases as the voltage increased. Such behaviors can be expressed as a strong self-passive process with the equilibrium of passive layer is driven from the dissolved to the forming side [36]. Along with the decrease in current, the metal dissolving is prohibited by the passive layer and continues to form and stabilizes. [37]

Above the Tafel region, the I-V curve is stable as with the voltage increased, there are no significant oscillation or metastable can be observed [5][6].

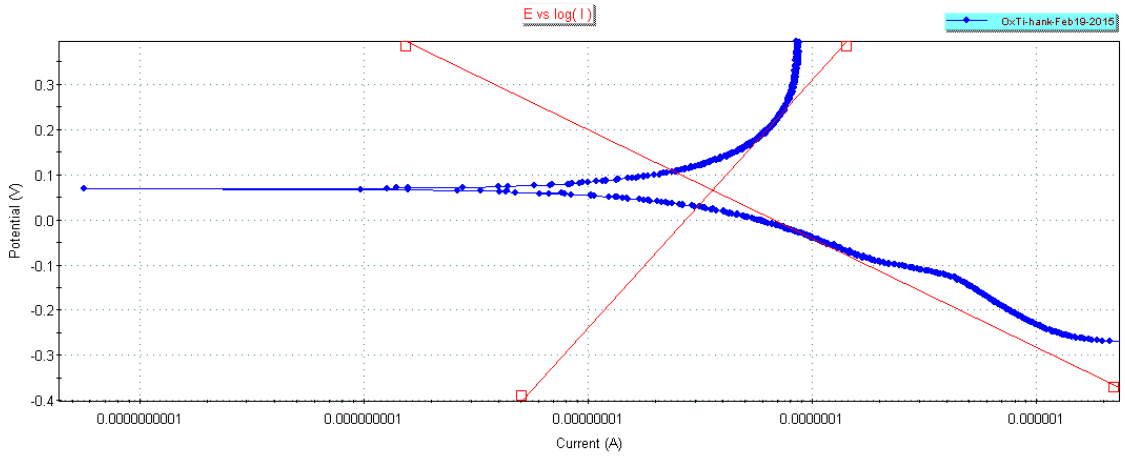

Figure 5.8 Tafel fit plot of PEO treated with oxide coating Titanium alloy Ti-6Al-4V.

5.2.4 PEO treated Titanium alloy Ti-6Al-4V with HA coating

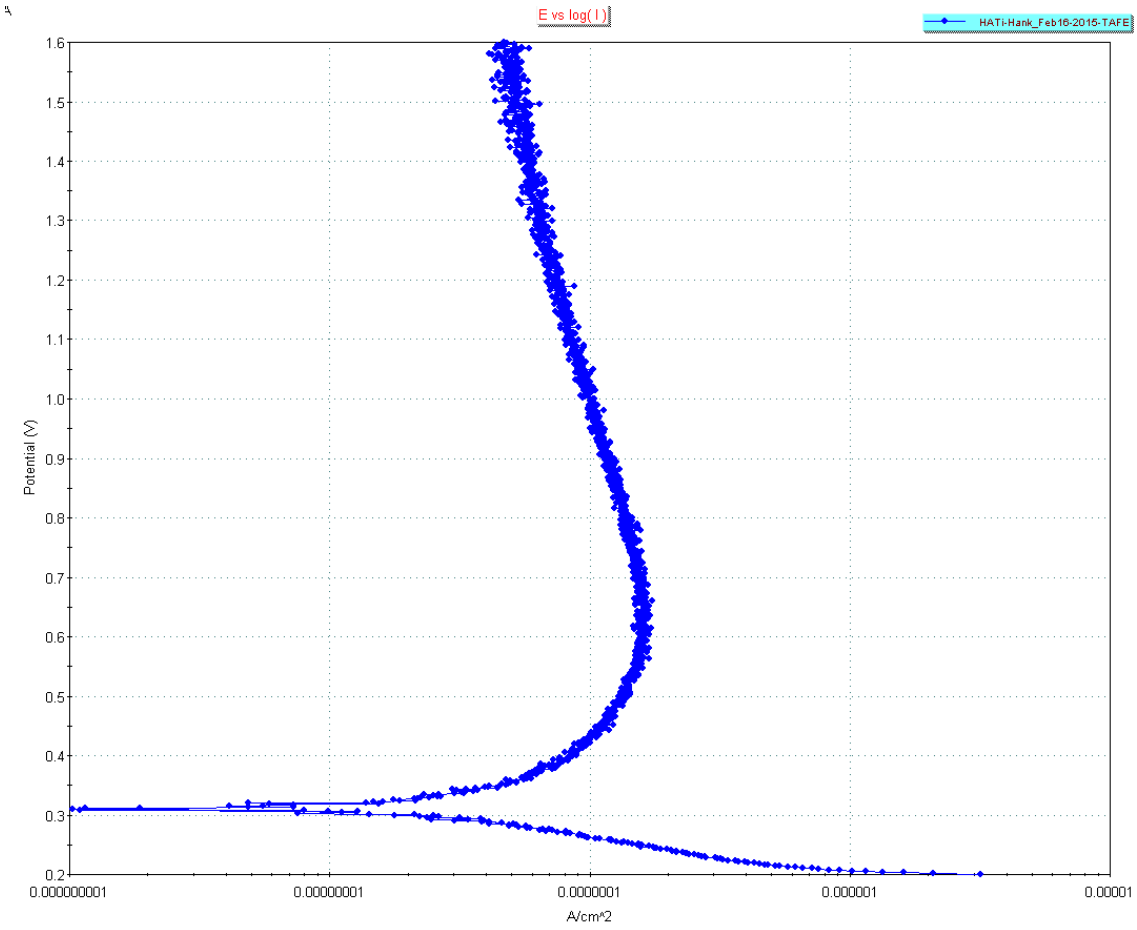

Figure 5.9 Potential dynamic plot of PEO treated Titanium alloy Ti-6Al-4V with HA coating.

Similar with the previous Figure, the HA coated sample shows a typical Tafel polarization pattern at cathodic to anodic polarization, but the corrosion potential is significantly elevated.

After the Tafel region, the slope of I-V curve is negative, in which the current decreases as the voltage increased. Such behaviors can be explained as a strong self-passive HA coating in the corrosive environment. The current density is the magnitude of chemical reaction between electrolytes – metal interface. As protected by HA coating, the metal surface is able to form metal oxide continuously. Thus the current decreases as the metal surface is oxidized and less electrons are exchanged [38].

Moreover, after the Tafel region, the passive region of the potential dynamic plot, the curve shows an oscillation in current as the voltage increases, of which the amplitude gains as the voltages rises. The reason for the oscillation is that the HA coating is a porous and honey net structure, in which the electrolyte - coating surface is far from ideal condition, thus the curve of potential dynamic is locally away from equilibrium [5][6].

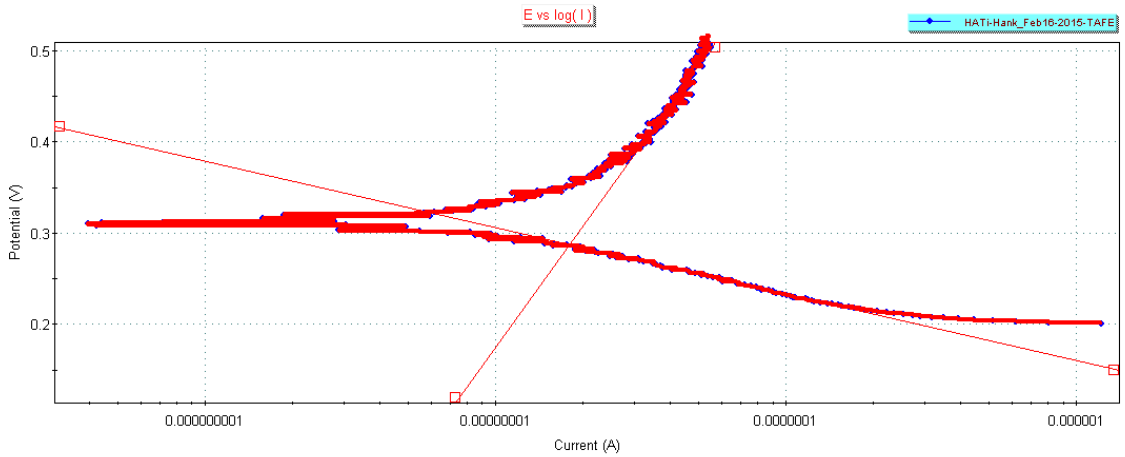

Figure 5.10 Tafel fit plot of PEO treated Titanium alloy Ti-6Al-4V sample with HA coating.

5.3 Electrochemical Impedance Spectroscopy

Electrochemical impedance spectroscopy, or in short EIS, is able to show the coating internal construction which other procedures can hardly accomplish. The oxide sample and HA coated sample are to be analyzed by EIS.

5.3.1 PEO treated Titanium alloy Ti-6Al-4V samples with oxide coating

The EIS results of PEO treated samples with oxide coating of Titanium alloy Ti-6Al-4V is shown in Figure 5.11.

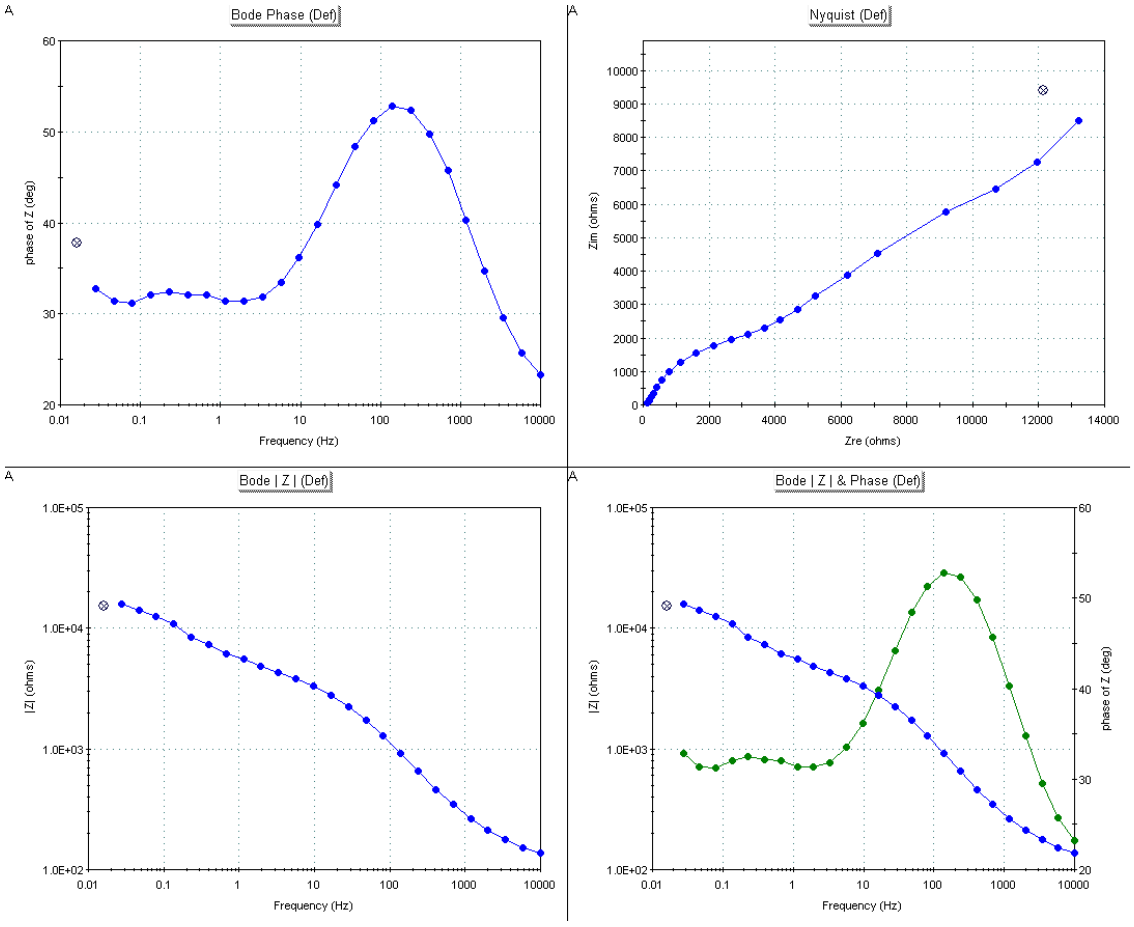

Figure 5.11 EIS data of PEO treated Titanium alloy Ti-6Al-4V sample with oxide coating.

The curve fitting of EIS data is shown in Figure 5.12.

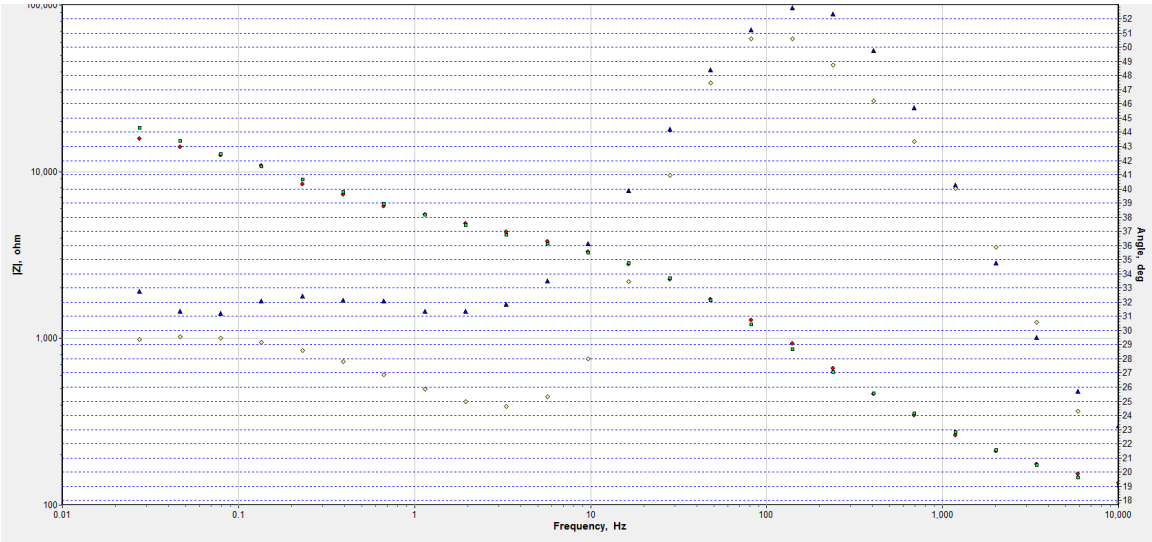

Figure 5.12 EIS curve fitting of PEO treated sample with oxide coating on Titanium alloy Ti-6Al-4V.

The equivalent circuit of PEO treated sample with oxide coating is shown in Figure 5.13.

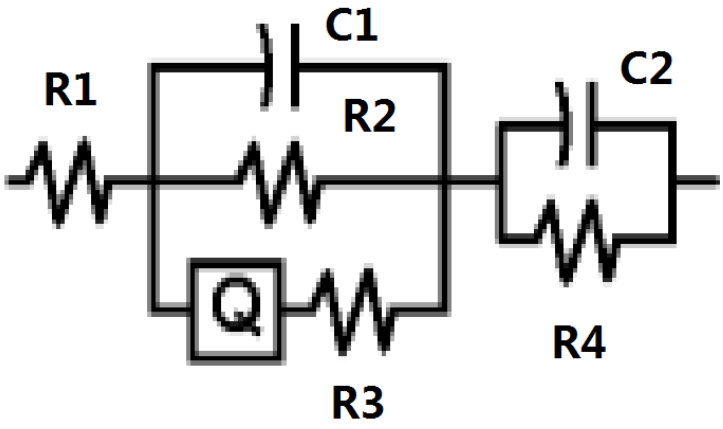

Figure 5.13 Equivalent circuit of PEO treated Titanium alloy Ti-6Al-4V sample with oxide coating.

The parameters of equivalent circuit of PEO treated sample with oxide coating are shown in Table 5.2

Table 5.2 List of Parameters of Equivalent Circuit

Parameter	Value
Resistance 1	112.5 Ω
CPE	0.001091
Resistance 2	1228 Ω
Capacitance 1	3.108×10^{-7} F
Resistance 3	0.01 Ω
Capacitance 2	3.496×10^{-6} F
Resistance 4	1673 Ω

The layer can be deduced from the equivalent circuit, shown in Figure 5.14.

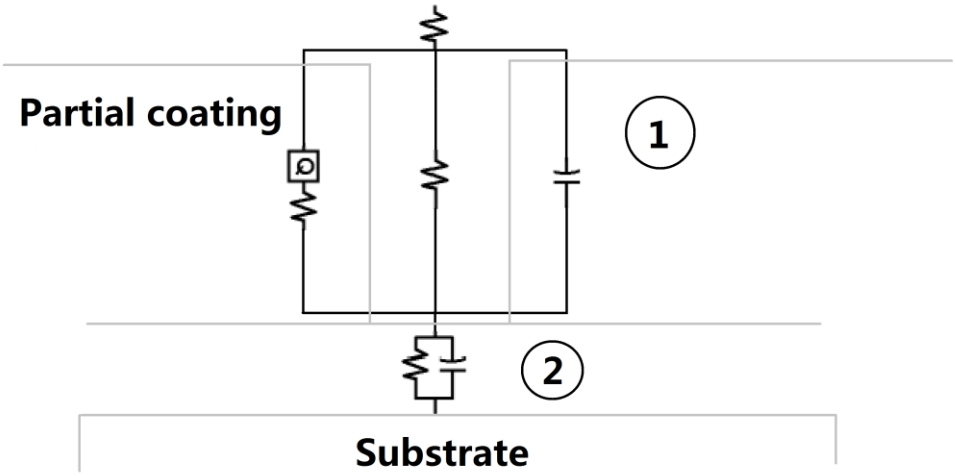

Figure 5.14 Coating structure represented by the equivalent circuit of PEO treated Titanium alloy Ti-6Al-4V sample with oxide coating.

The first electrical element in the circuit is a resistor. For the electrolyte is conductivity is used and it represents the electrical potential drops by electrolyte.

There are two layers of coating in the oxide coated sample.

The first layer is a partial coated oxide layer; the resistor 2 existing is to show there

an uncovered area which results in a direct contact between uncoated areas and electrolyte.

The series connected constant phase element and resistor in the partial coating part of Figure 5.3.3.2 indicates a tunneling leaking, which has a partial conductive and partial diffusion path.

The base layer is another oxide layer. Even with a resistor in it, the second layer is not leaked or exposed. The base layer is a mixture structure of conductive crystal structure and non-conducting amorphous structure. Those mixing result a conductive - dielectric behavior layer [7].

5.3.2 PEO treated Titanium alloy Ti-6Al-4V sample with HA coating

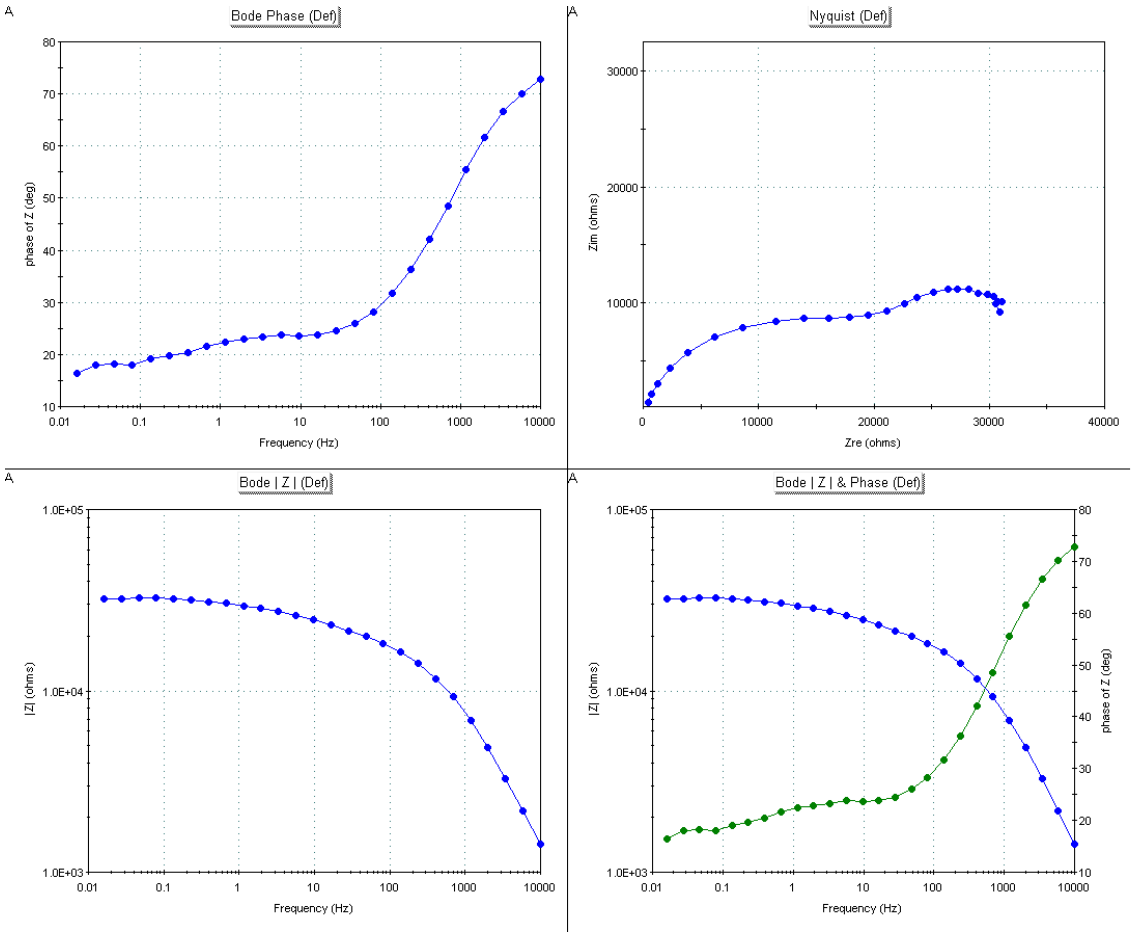

Figure 5.15 EIS data of PEO treated sample of oxide coating on Titanium alloy Ti-6Al-4V.

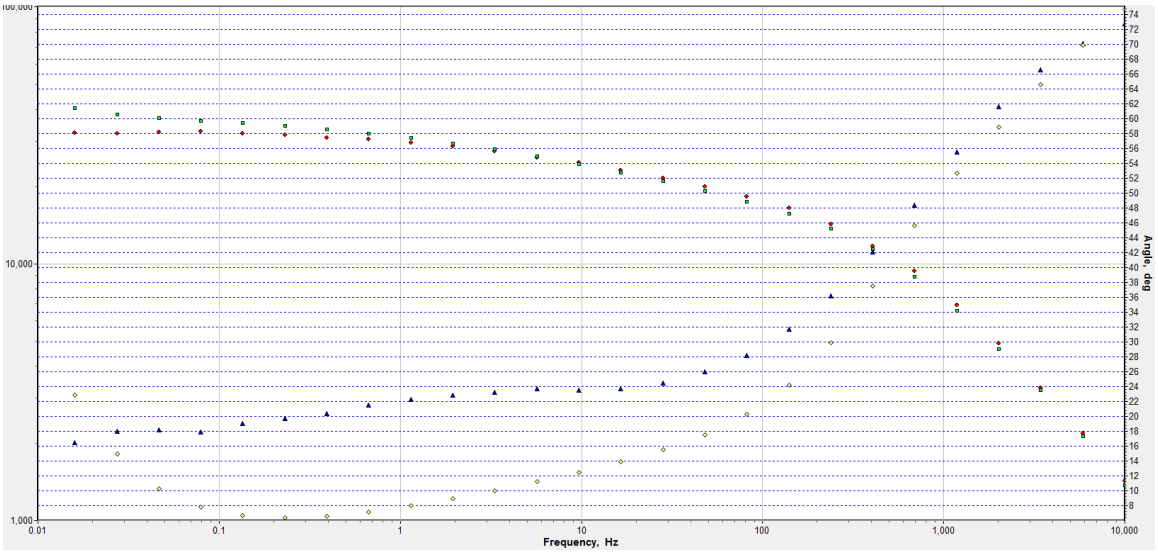

Figure 5.16 EIS curve fitting of PEO treated sample of oxide coating on Titanium alloy Ti-6Al-4V.

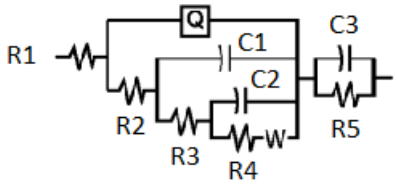

Figure 5.17 Equivalent circuit of PEO treated sample of oxide coating on Titanium alloy Ti-6Al-4V.

The parameters of equivalent circuit are shown in Table 5.4.

Table 5.4 List of Parameters of Equivalent Circuit

Parameter	Value
Resistance 1	89.24 Ω
CPE	3.367×10^{-5}
Resistance 2	7885 Ω
Capacitance 1	9.262×10^{-5} F
Resistance 3	$1.138 \times 10^{4}\Omega$
Capacitance 2	5.156×10^{-4} F
Resistance 4	$4.113 \times 10^{-4}\Omega$
Warburg	6.247×10^{-13}
Capacitance 3	4.226×10^{-6} F
Resistance 5	958.9 Ω

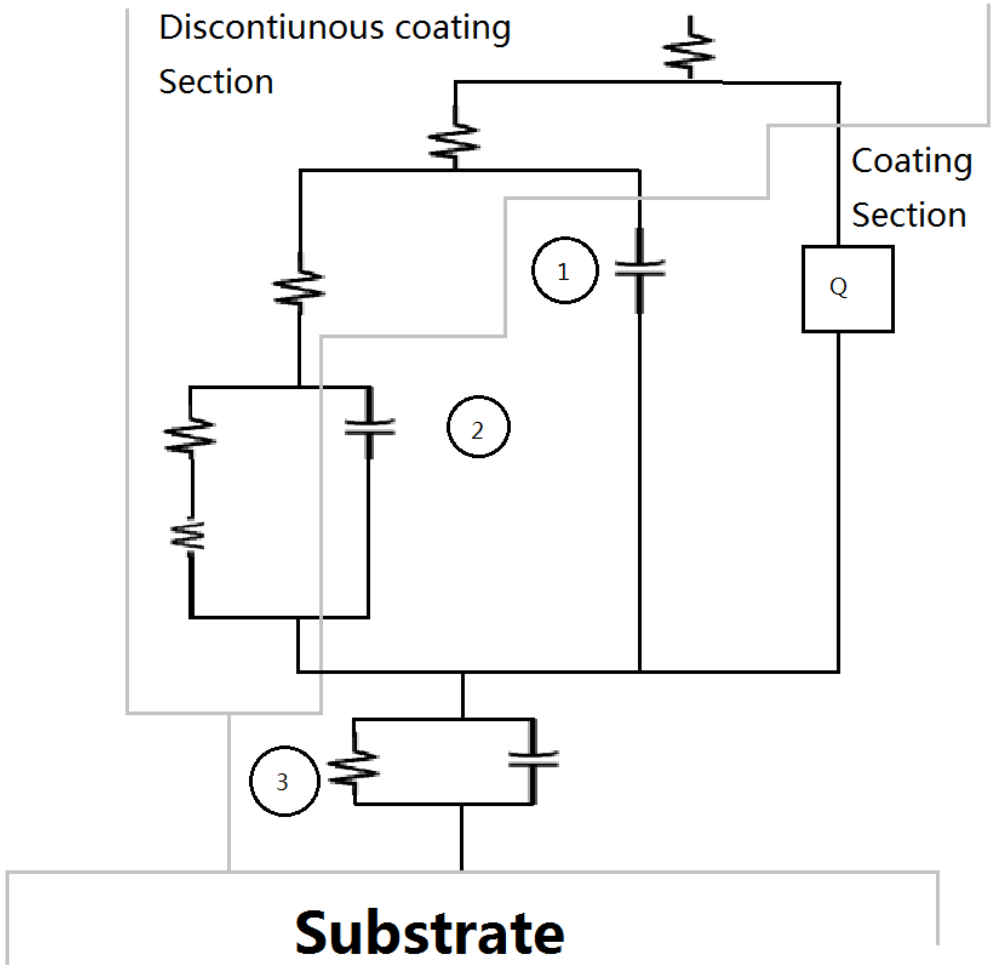

Figure 5.18 Coating structure represented by the equivalent circuit of PEO treated sample of HA coating on Titanium alloy Ti-6Al-4V.

The coating structure which can be inferred from equivalent circuit is shown in Figure 5.18. The presumed coating structure shows three layer of coating micro structure, numbered with 1, 2, and 3 in Figure 5.18.

The first electrical element in the circuit is the resistor, which represents the electrical potential drops by electrolyte. For the electrolyte conductivity is used and the resistor represents the IR drop of electrolyte.

The first two layers, 1 and 2, shown in Figure 5.18, are partly coating layer, in which the resistors can be found in these two layers, indicating the two layers consist of leaking of imperfect. As the leaking is filled with electrolyte, it becomes partial conductor and partial dielectric. Such layer is HA porous layer with hole and pits [39].

In the third layer, 3, there is a dense oxide layer in base of HA coating. The base layer consists of parallel connected resistor and capacitor. However, the resistor is not resulting from leaking coating, but the partial crystal structure of oxide layer during the oxide layer forming. As the parallel connected resistor and capacitor existed, the third layer is connected by the crystal structure which is conductive and the oxide layer which is dielectric. [40]

Also, because the HA coating is porous, there is a constant phase element which connects the electrolyte and the third layer, marked with Q in the Figure 5.18. For the porous structure of HA, the electrolyte fills the pores in the HA, thus creates a tunnel like diffusion zone, which result in a constant phase element behavior. The constant phase element can be considered as leaking in the EIS, but in case, this structure is electrical conductive [7].

5.4 Corrosion Test Results

According to Faraday's Law the corrosion rate can be calculated by [5]:

$$R=0.129\frac{ai}{nD} \tag{5.1}$$

Where i is the corrosion current, D is the density, n is the numbers of electron

transferred, and α is the atomic weight.

The results of corrosion potential, corrosion current and corrosion rate are shown in Table 5.4.

Table 5.4 List of Corrosion Potential, Corrosion Current and Corrosion Rate

Material of Samples	**Corrosion potential (mV)**	**Corrosion Current ($\mu A/cm^2$)**	**Corrosion Rate (mpy)**
Titanium Grade 2	-11.69	0.2323	0.046
Titanium Grade 5(Ti6Al4V)	-302.598	0.4588	0.088
Titanium Grade 5 with oxide coating	65.746	0.036	0.0075
Titanium Grade 5 with HA coating	299.98	0.0119	0.0026

The corrosion rate is reduced by the coating as can be seen from the Table 5.4; also the corrosion potential is raised by the coating, thus give the metal more resistance to corroding.

CHAPTER 6

CONCLUSIONS AND FUTURE WORK

6.1 Conclusions

One of challenge in contemporary bio-material development is to increase the corrosion resistance of bio-material [41][42]. As a novel surface treatment of metallic material, the plasma electrolytic oxidation is able to meet such challenges by the conclusions from this thesis:

1. The surface characterization shows that a uniform coating is formed on the surface of substrate.

By the result of optical imaging and SEM imaging, the oxide coating by PEO method is dense and uniform throughout the surface of the substrate. The HA coating by PEO method is porous and free of defect throughout the surface of the substrate.

2. By the results of XRD, the oxide coating by PEO method is a ceramic coating with amorphous structure. The HA coating by PEO method is a partial crystal structure with HA crystal among with it. The thickness of HA coating is 60 μm.
3. The coating of PEO method increases corrosion resistance of the substrate material.

By comparing coated and uncoated samples the corrosion potential is increased by the PEO coating. The corrosion potential of uncoated Titanium alloy is -302.598 mV, lower than the corrosion potential of pure Titanium Grade 2, which is -11.69 mV. The corrosion potential of PEO treated sample with oxide coating is 65.746 mV and the corrosion potential of PEO treated sample

with HA coating is 299.98 mV, which the coated samples show a significant increase in corrosion resistance.

The corrosion current is decreased by the PEO coating, from the uncoated sample of Titanium alloy, which is 0.4588 $\mu A/cm^2$, to 0.036 $\mu A/cm^2$ which is the corrosion current of sample with oxide coating, and to 0.0119$\mu A/cm^2$, which is the corrosion current of sample with oxide coating. The decreased corrosion current indicates that there would be less ion releasing which comes from the corroding of material, and less corrosion damaging to the surface of material in vitro.

Also the corrosion rate is reduced from 0.088 mpy of for samples without coating, to 0.0075 mpy for samples with oxide coating, and to 0.0026 mpy for samples with HA coating.

4. A corrosion resistant coating with multi-layer micro-structure is formed by the PEO method.

The corrosion resistant microstructure is clarified by EIS. Multi-layer formation has been formed by PEO method in both samples with oxide coating and HA coating.

In the sample with oxide coating, a double layer oxide coating is formed. The substrate is partial covered by first layer of coating, and the second layer is dense and fully covering the surface of substrate. In the sample with HA coating, there are three layers coating formed. The first two layers are porous and the third layer which is connecting the substrate and the outer layer is dense. The three layers reduce the electrolytic-metal chemical reactions significantly.

This multi-layer coating protects the substrate from the corroding environment and thus increasing the corrosion resistance, which can be seen in the previous discussion of corrosion potential and corrosion rate.

6.2 Future Work

The characterization of PEO coating on the Titanium alloy is the first step of applying PEO method into the real industrial application of bio-material surface treatment [43][44], there are extensive works to be done in the future:

1. More PEO coating study on different kind of substrates other than Titanium alloy Ti-6Al-4V needs to be done. Such as Titanium Grade 2 is one of the best candidates in Titanium alloy family for biomedical engineering [45]. A study on PEO surface treatment for Titanium Grade 2 and other Titanium alloys needs to be carried out, to see if there are improvements on such alloys.[46]
2. The Hank solution can be replaced by other kinds of simulated body fluid, such as artificial saliva, in order to see if the PEO coating is able to increase the corrosion resistance of dental implant. [47] [48]
3. The stress-corrosion test has not been carried out; however, the stress-corrosion is one of major corrosion effect taking place in vivo. So further work should be focus on how the stress effects the corrosion of bio-material [48].
4. Moreover, the experiment of in vivo needs to be done by a series of animal test, to check if the PEO sample is able to fit the requirements of really in vivo environment [49] [50] [51].

REFERENCES

1. R. Narayan / *Biomedical Materials*. (2009) Springer Science Business Media, LLC, 233 Spring Street, New York, NY 10013.

2. M. Mucalo / Hydroxyapatite (HAp) for Biomedical Applications. (2015) Elsevier Business Intelligence (Corporate Office) 685 Route 202/206 Second Floor, Bridgewater, NJ 08807

3. W. L. Jaffe et al. / NEW YORK, N.Y. J Bone Joint Surg Am, 1996 Dec; 78 (12): 1918 -34.

4. L. Besra, M. Liu / Progress in Materials Science 52 (2007) 1–61

5. D.A. Jones / Principles *and Prevention of Corrosion*. (1996) (2nd edition). Prentice Hall, Upper Saddle River, NJ, 07458.

6. P.N. Chavan et al. / Materials Science and Engineering B 168 (2010) 224–230

7. R.W. Revie / Corrosion *and Corrosion Control*. (2007) (4th Edition). 111 River Street, Hoboken, NJ 07030-5774.

8. M.E. Orazem / *Electrochemical Impedance Spectroscopy*. (2008) 111 River Street, Hoboken, NJ 07030-5774.

9. A. Nominé et al. / Surface & Coatings Technology. (2015)

10. S. Hiromoto / *The Electrochemical Society Interface • Summer (2008).* 41-44.

11. S. Durdu et al. / Journal of Alloys and Compounds 551 (2013) 422–429

12. Y. Han et al. / Electrochemistry Communications 10 (2008) 510–513

13. L.P. Faverani et al. / Materials Science and Engineering C 43 (2014) 1–10

14. C.S. Dunleavy et al. / Surface & Coatings Technology 206 (2011) 1051–1061

15. V. Ozhukil Kollath et al. / Journal of the European Ceramic Society 33 (2013) 2715–2721

16. M. Mohedano et al. / Journal of Biomedical Materials Research B: applied biomaterials (2013) 101B:1524–1537.

17. S. Abbasi et al. / Materials Science and Engineering C 33 (2013) 2555–2561

18. S. Han et al. / Tissue Engineering and Regenerative Medicine, (2010) Vol. 7, No. 3, pp 338-343

19. A.Kossenko et al. / Glass Physics and Chemistry, 2013, Vol. 39, No. 6, pp. 639–642. © Pleiades Publishing, Ltd., 2013.

20. A. Kazek-Kęsik et al. / Materials Science and Engineering C 43 (2014) 172–181

21. Y. Han et al. / Electrochemistry Communications 10 (2008) 510–513

22. M.-S. Kim et al. / Electrochemistry Communications 9 (2007) 1886–1891

23. L Rodriguez et al. / Journal of Biomedical Materials Research B: applied biomaterials | Jul 2014 vol 102b, issue 5

24. A. Lugovskoy et al. / Materials Science and Engineering C 43 (2014) 527–532

25. A.L. Yerokhin et al. / Surface and Coatings Technology 122 (1999) 73–93

26. J.M. Wheeler et al. / Surface & Coatings Technology 204 (2010) 3399–3409

27. E.V. Parfenov et al. / Surface & Coatings Technology 201 (2007) 8661–8670

28. A. L. Yerokhin et al. / Ceramics International 24 (1998) l-6

29. L. Zhang et al. / Corrosion Science 91 (2015) 7–28

30. Y. Gao et al. / Electrochimica Acta 149 (2014) 218–230

31. J. Martin et al. / Surface & Coatings Technology 269 (2015) 36–46

32. Z. Yao et al. / Surface & Coatings Technology 242 (2014) 146–151

33. M.R. Garsivaz jazi et al. / Surface & Coatings Technology 244 (2014) 29–36

34. J. Dean et al. / Surface & Coatings Technology 269 (2015) 47–53

35. V. Dehnavi et al. / Surface & Coatings Technology 269 (2015) 91–99

36. Y. Qin et al. / Surface & Coatings Technology 269 (2015) 266–272

37. X. Yu et al. / Surface & Coatings Technology 269 (2015) 30–35

38. S. Durdu, M. Usta / Ceramics International 40 (2014) 3627–3635

39. A. Tahmasbi Rad et al. / Ceramics International 40 (2014) 12681–12691

40. H.-Y. Wang et al. / Materials Science and Engineering C 42 (2014) 657–664

41. S. Durdu et al. / Journal of Alloys and Compounds 551 (2013) 422–429

42. K.M. Lee et al. / Journal of Alloys and Compounds 615 (2014) S418–S422

43. M. Montazeri et al. / Applied Surface Science 257 (2011) 7268–7275

44. K.R. Shin et al. / Applied Surface Science 314 (2014) 221–227

45. J. Wu et al. / Applied Surface Science 316 (2014) 102–107

46. R. Liu et al. / Materials Chemistry and Physics 148 (2014) 284-292

47. H.E. Achneck. et al. / Biomaterials 32 (2011) 10-18

48. L.O. Snizhko / Protection of Metals and Physical Chemistry of Surfaces, 2014, Vol. 50, No. 6, pp. 705–708

49. E.W. Collings / The Physical Metallurgy of Titanium Alloys, American Society for Metals, 1984, pp. 2

50. L. Wang / Journal of Electrochemical. Society. 2014 volume 161, issue 1, C20-C24

51. S. A. Alves / Special Issue: LUBMAT 2012 - Lubrication, Maintenance and Tribotechnology Volume 26, Issue 7-8, pages 500–513, November-December 2014